glc7-E101Q is a novel tool for integrated genomic and proteomic analysis of PP1/Glc7 phosphatase functional networks in *Saccharomyces cerevisiae*

by

Nicolas Szapiel

A thesis submitted to
The Faculty of Graduate Studies and Research
In partial fulfillment of the requirements for the
Degree of Master of Science

Department of Biology
McGill University
Montréal, Québec, Canada

Submitted May 2007

Your file Votre référence
ISBN: 978-0-494-32793-7
Our file Notre référence
ISBN: 978-0-494-32793-7

Abstract

Reversible phosphorylation is a major mechanism for regulating the activity, localization and stability of proteins required for vital cellular processes such as glucose metabolism, gene expression, establishment of polarity, mitosis and cytokinesis. Phospho-regulation is driven by the activities of kinases and phosphatases. Together, these enzymes account for ~3% of eukaryotic genomes and it is estimated that 30% of the eukaryotic proteome is composed of phospho-proteins. Protein kinases (PKs) have been studied extensively, however relatively little is known regarding the signaling networks of protein phosphatases (PPases). The identification of PPase functional networks has been slow due to the redundant nature of the majority of PPases, the complexity of their substrate recognition *in vivo*, and the lack of large-scale analyses that would facilitate network analysis. We hypothesized that large-scale analysis of genetic interactions using the Synthetic Genetic Array (SGA) and proteomic analyses using 2D-PAGE Difference Gel Electrophoresis (DiGE) could reveal PPase functional networks. Here, we apply this approach to the essential and conserved PP1 PPase Glc7 as it regulates numerous cellular processes in budding yeast. For this study, we created a *glc7* hypomorphic mutant (*glc7-E101Q*) suited for both SGA and DiGE analyses. SGA analysis of *glc7-E101Q* revealed a broad network of 147 synthetic sick/lethal (SSL) and 178 synthetic rescue (SR) interactions. DiGE comparison of the *glc7-E101Q* proteome relative to wild-type at medium-resolution (~1000 proteins) revealed alterations in 39 proteins that changed as a consequence of both the mutation and growth conditions. One of the proteins identified in this analysis was Eno1, a non-essential enolase that is mis-regulated in the presence of glucose and identified a SR mutation in the *glc7-E101Q* SGA. Subsequent phenotypic analysis suggests a novel, non-metabolic role for Eno1 in the Glc7 interaction network. Our results reveal that parallel analysis, using SGA and DIGE, can reveal novel functions and networks that a single analysis may not detect.

Résumé

La phosphorylation est un important mécanisme de contrôle de l'activité, localisation et stabilité des protéines requises pour des processus vitaux tels que: le métabolisme, l'expression, l'établissement de la polarité, la mitose et la cytokinèse. La phospho-régulation dépend sur l'activité de protéines kinases (PKs) et phosphatases (PPase). Ces deux classes d'enzymes forment ~3% du génome des eucaryotes et il est estimé que ~30% du protéome des eucaryotes est composé de phospho-protéines. Les PKs ont été étudiées abondamment, mais relativement peu est connu sur les réseaux de signalisation de PPases. L'identification de ces réseaux est ardue à cause de la complexité des interactions entre les PPases et leurs substrats, ainsi que dû à la rareté d'analyse à grande échelle de ces réseaux. Nous avons supposé qu'une analyse à grande échelle des interactions génétiques utilisant le *Synthetic Genetic Array* (SGA) combinée avec une approche protéomique utilisant le *2D-PAGE Difference Gel Electrophoresis* (DiGE) pourrait élucider des nouvelles composantes de ces réseaux. Nous avons appliqué cette méthodologie à Glc7, une PPase essentielle de type PP1 qui joue un rôle dans plusieurs processus cellulaires. Nous avons créé un mutant catalytique de *GLC7* (*glc7-E101Q*), approprié pour le SGA et le DiGE. Le SGA a révélé un large réseau d'interactions génétiques: 147 synthétiques malades/létales (SSL) et 178 restaurations synthétiques (SR). Les comparaisons du protéome de *glc7-E101Q* avec la souche sauvage en utilisant le DiGE (résolution ~1000 protéines) ont révélé des changements dans 39 protéines, dû à la mutation et les conditions de croissance. Une de ces protéines est Eno1, un composant de l'énolase, dont la régulation a été anormale en présence de glucose (DiGE). Eno1 a aussi été identifié comme un SR de l'allèle *glc7-E101Q* par le SGA. Ces résultats suggèrent un nouveau rôle, pour Eno1 dans le réseau de signalisation de Glc7. Nos résultats démontrent qu'une analyse combinant SGA et DIGE peut révéler des nouvelles fonctions qu'une seule analyse ne peut détecter.

Acknowledgements

I thank my supervisor, Dr. Jackie Vogel for her guidance and mentorship over the years and for giving me the opportunity to pursue my scientific interests under her valuable supervision. I am also very grateful to Dr. Paul Harrison and Dr. Martin Latterich, members of my graduate committee, for their insightful comments and suggestions and to Dr. Howard Bussey for helping to initiate the project and sharing his vast expertise with the Vogel Lab.

I thank James Knockleby, Lara Cuschieri and Michael Logan for their advice and help on and off the bench as well as for their great camaraderie during all these years. Thanks also to past and present Vogel lab members who have contributed to this ambitious project: Marc Edwards, Zineb Mounir, Mike Neszt, Thao Nguyen and Hanting Por- who also kept everything running in the lab during this time. I would also like to thank the CIAN staff for their expertise and technical advice: Guillaume Lesage, Elke Küster-Schöck and Scott Bunnell.

Finally, I would like to thank my Mother and my Sister as well as the rest of my family for their Love and constant help, and finally Diana Roopchand for her faithful support and Love.

Preface

In compliance with the "Guidelines Concerning Thesis Preparation" of the Faculty of Graduate Studies and Research of McGill University, Chapter 2 of this thesis represents the text of a paper submitted to the journal *Molecular and Cellular Biology* (February 1st, 2007; MCB00197-07 Version 1).

Contribution of Co-Authors

This thesis is written in manuscript style and was prepared with my supervisor.

Chapter 1: This chapter was written with minimal input from my supervisor.

Chapter 2: This chapter was written in manuscript format with my supervisor and co-author Michael Logan, and has been submitted to the journal *Molecular and Cellular Biology* (February 1st, 2007; MCB00197-07 Version 1). My contributions to this study were the following:

1) Modeling of Glc7 based on human PP1.
2) Mutagenesis of Glc7, resulting in the *glc7-D91N* allele (YNS19) and the *glc7-E101Q* allele (YNS53). Preparation of wild type and mutant Glc7 Protein A fusion proteins (YNS23, YNS26, YNS27, YNS44), rescue constructs and the rescue allele *GLC7-res* (YNS128), and preparation of the SGA query strain (YNS98).
3) Assessment of growth (on glucose versus glycerol), cell cycle progression of the *glc7-E101Q* strain (bud index, FACS), stability of the Glc7-E101Q-ProA fusion protein.
4) Defects in glucose metabolism and glycogen accumulation of the *glc7-E101Q* mutant and rescue by *GLC7-res*.
5) Multiplexed 2D-DiGE analysis of Glc7 and carbon source dependant changes in the proteome at medium resolution (980 spots), and spot excision for Eno1 MS.

The analysis of synthetic genetic interactions of the *glc7-E101Q* mutant (SGA analysis) was performed by Thao Nguyen and Michael Logan. Network analysis was performed by Michael Logan, Thao Nguyen and Guillaume Lesage.

Chapter 3: This chapter was written with minimal input from my supervisor.

List of Figures

List of Tables

List of Abbreviations

1-DE – 1 dimensional electrophoresis

2-DE – 2 dimensional electrophoresis

aa – amino acid(s)

bp - base pair(s)

C - terminal - carboxyl terminal

CDK – cyclin-dependent kinase

CM – catalytic mutant

DNA – deoxyribonucleic acid

DP - Deep Purple protein stain (GE)

DTT - Dithiothreitol

ECL – enhanced chemiluminescence

FACS – fluorescence-activated cell sorting

G1 – gap phase before S phase

G2 – gap phase before M phase

GFP – green fluorescent protein

K_{cat} – catalysis rate

kD – kilodalton

K_m – Michaelis-Menten equilibrium constant

M phase – mitotic phase

MAPK – mitogen-activated protein kinase

MEN – mitotic exit network

MPF – mitosis promoting factor

mRNA – messenger RNA

MS – mass spectrometry

N-terminal - amino terminal

PTMs – post-translational modifications

PK – protein kinase

PPASE – phosphatase

SPB – spindle pole body

SL – synthetic lethal genetic interaction (SGA)

SR – synthetic rescue genetic interaction (SGA)

SS - synthetic sick genetic interaction (SGA)

WT – wild type

Epigraph

"If you give up every time you don't achieve the immediate gain you want, you're just guaranteeing that the worst is going to happen."

Noam Chomsky
Imperial Ambitions

Chapter 1: Introduction

1.1. Cellular regulation: protein kinases and phosphatases

The eukaryotic cell relies on a diverse set of mechanisms for the regulation of important cellular processes such as DNA replication, mitosis, metabolism, and gene expression. To great extent, this control is achieved by regulating the activity of proteins involved in these processes; either by modulating their expression, or through post-translational modifications that directly impact their function, localization or stability. For example, progression through the cell cycle is driven by changes in the activity of different forms of cyclin-dependant kinases (Cdks). The differential activity of Cdk is controlled by both the cell cycle-dependant expression and degradation of specific cyclins and a complex set of inhibitory or activating phosphorylation events at highly conserved Cdk residues. The transcriptional and post-translational regulation of Cdk activity during the cell cycle is a classic example of the inter-dependant roles of transcriptional and post-translational modification, and demonstrates the complexity of intra-cellular signaling and control. (Dynlacht, 1997; Ferrari, 2006; Thornton and Toczyski, 2006).

Whereas transcription, translation and degradation are irreversible regulatory mechanisms, phosphorylation is reversible. Phospho-regulatory networks are composed of protein kinases (PKs) and phosphatases (PPases). PKs phosphorylate target proteins at specific serine, threonine or tyrosine residues and PPases counteract the action of PKs by removing the phosphate groups. In combination, PKs and PPases can rapidly activate or inhibit specific pathways without *de novo* synthesis of its components. Indeed, it is estimated that 30% of the eukaryotic proteome is composed of phospho-proteins (Barford, 1995). First generation integrative phosphorylation maps based on proteome chip technology, protein-protein interactions and transcription factor binding

data from the budding yeast *Saccharomyces cerevisiae* confirm this ratio. Budding yeast contains approximately ~5700 ORFs encoding known or uncharacterized proteins (SGD). Recent efforts using an array containing ~4 400 spotted proteins revealed over 4000 phosphorylation events involving 1325 different proteins (Ptacek et al., 2005). This result represents 30% of proteins present in the array and despite the limited coverage of the array, suggests that at least 23% of the entire proteome is phosphorylated.

Phospho-regulation has profound effects on the targeted protein's activity and properties. At the intra-molecular level, reversible phospho-regulation of specific residues may induce allosteric conformational changes that translate into changes in activity or function (Johnson and O'Reilly, 1996). For example, in the case of kinases, phosphorylation of serine, threonine or tyrosine residues in the activation segment within the catalytic domain is a common mechanism of their activation (Nolen et al., 2004). In contrast, inhibitory phosphorylation confers either a conformational change that blocks binding of a substrate to a catalytic site or imparts a negative charge that reduces binding efficiency (Johnson and O'Reilly, 1996). At the inter-molecular level, phospho-regulation may promote an event, such as the conjugation of ubiquitin moieties at lysine residues. Additionally, it is an important regulatory mechanism in the formation of protein-protein interactions (Barford, 1995). Phospho-regulation is central to numerous vital cellular functions; the study of the entire phosphorylation machinery is therefore key to understanding cellular processes, though it remains difficult to dissect in detail. For example, through association with distinct regulatory subunits, protein phosphatase 1 (PP1) plays a role in metabolism, the relaxation of actomyosin fibers, the return to basal patterns of protein synthesis and the down-regulation of ion pumps and transporters in various ion channels involved in the excitation of neurons (Ceulemans and Bollen, 2004; Hu et al., 2006). These PP1 functions are unconnected phenotypically, and the regulatory role of PP1 in these processes is poorly understood as in some cases PP1

may act as a positive regulator and in others as an inhibitor. Nonetheless, breakdowns in the phospho-regulatory networks clearly underlie diseases such as diabetes, cancer and disorders of the immune and cardiovascular systems, making PPases prime targets for drug discovery (Kuruma et al., 2005; Pawson, 1995; Stark, 1996; Van Hoof and Goris, 2003; Ventura and Nebreda, 2006).

More specifically, glucose metabolism is impacted on by changes in phosphorylation state of key proteins that control carbohydrate usage and storage. All eukaryotes share the ability to adapt their metabolism for optimal utilization and management of carbon sources available in the environment. In the case of the unicellular budding yeast, glucose is the preferred carbon source. Expression analysis has shown that ~40% of the genome has glucose-dependent expression profiles (Santangelo, 2006). The presence of glucose induces the transcription of genes involved in glycolytic pathways and represses expression of genes regulating gluconeogenic pathways. This shift in genome expression is achieved via direct phosphorylation and transcriptional control of metabolic enzymes. Mutations affecting the metabolic phospho-regulatory network regulating glucose repression (such as the PP1 ortholog in budding yeast), results in reduced fitness, increased sensitivity to starvation and highly reduced growth on non-fermentable carbon sources (Carlson, 1999; Ceulemans and Bollen, 2004; Francois and Parrou, 2001; Parrou et al., 1997; Sakumoto et al., 2002). In mammals, although the control of metabolic pathways is significantly more complex, glucose metabolism relies on similar mechanisms. Studies on rat hepatocytes have shown that insulin-dependent diabetes is linked to impaired glucose-induced activation of glycogen metabolism due to defective phospho-regulation by PP1 (Bollen and Stalmans, 1992). Moreover, abnormally high activation of glycogen metabolism in rats with hyper-thyroidism appears to be caused by increased levels of the same key phospho-regulatory activator (PP1) of glycogen metabolism (Lavoie et al., 1999).

PPases account for less than ~1% of all eukaryotic genes and can be classified into three main groups and less than ten subfamilies according to the conservation of the catalytic motifs and their ability to dephosphorylate serine/threonine and/or tyrosine residues (Ceulemans et al., 2002). Protein PPases are commonly found to be 2-5 times lower in their complexity than PKs (Bollen, 2001; Ceulemans and Bollen, 2004; Ducruet et al., 2005). This difference is even more pronounced when limiting the analysis to serine/threonine specific PKs and PPases, where this ratio is as high as ~ 20:1, particularly in higher vertebrates. Bioinformatic analysis of the human genome estimates the number of PPases to be ~100 (Ducruet et al., 2005) and is predicted to only encode ~20 serine/threonine PPases (Ceulemans et al., 2002). Clearly, while the number of PKs has steadily increased during eukaryotic evolution with the development of novel processes requiring regulation such as immunity, angiogenesis and haematopoieses, PPases lagged in number and employed another evolutionary strategy to cope with the expanding eukaryotic phosphoproteome.

PPases function as holoenzymes where the catalytic subunit associates with specific adaptor proteins. Adaptor proteins can modulate enzyme activity, dictate substrate specificity and in some cases act as a substrate of a particular PPases (Ceulemans and Bollen, 2004). Regulatory subunits are a subcategory of adaptor proteins that promote substrate specificity and/or targeting. Therefore, the true diversity of PPases is achieved with the expansion of adaptor subunits. As holoenzymes, PPases show similar diversity to kinases (Ceulemans and Bollen, 2004). For example, mammalian protein phosphatase 2A (PP2A) is a trimeric serine/threonine phosphatase composed of a catalytic (C) subunit (2 isoforms) bound to a structural A subunit (2 isoforms) and one of several regulatory B subunits (~20 isoforms) (Janssens and Goris, 2001). The A subunit acts as a scaffold for the B and C subunits. Interestingly the AC core enzyme lacks substrate specificity, which is provided by the regulatory B subunit

that alters access to the catalytic site and may also promote the localization of the core enzyme to particular sub-cellular compartments (Janssens and Goris, 2001). In general, the binding of regulatory subunits is mutually exclusive, suggesting one or more overlapping binding sites to the core enzyme and regulatory subunit outside of the catalytic domain, creating multiple points of contact (Barford et al., 1998). However, few robust binding motifs have been identified due to low homology between the regulatory subunits of different eukaryotic taxonomies making identification and study of new PPase regulatory functions difficult.

PKs account for ~2% of all eukaryotic genes (Bollen, 2001). Using predicted catalytic motifs, 478 putative eukaryotic PKs are present in the human genome making them one of the largest protein "superfamilies" (Ferrari, 2006). This number does not include the ~40 poorly characterized atypical PKs that do not show the conserved catalytic motifs seen in other phospho-transferring enzymes (Hanks, 2003).

The human kinome is complex with eight major groups and several families and subfamilies of kinases that selectively phosphorylate serine/threonine or tyrosine residues, although other residues may also be targeted. The canonical catalytic domain of eukaryotic PKs is composed of twelve sub-domains containing conserved catalytic residues creating a bi-lobate tertiary structure. The N-terminal lobe is composed mostly of beta sheets (catalytic sub-domains 1 to 4) and binds ATP whereas the larger C-terminal lobe is composed exclusively of alpha helices (catalytic sub-domains 6A/B to 11) and mediates substrate recognition along with the phospho-transfer reaction. Structurally, the ATP moiety resides in a deep cleft between the two lobes and is partially shielded by a regulatory peptide called the activation segment, which contains one or two phosphorylation sites that are critical for regulation of catalytic activity and recruitment of ATP. Phosphorylation of the activation segment along with binding of

accessory proteins (as in the case of Cdk1) induces major conformational changes: opening of the bi-lobal structure, rearrangement of secondary structural elements and reorganization of the activation segment (Johnson and Lewis, 2001). These structural changes lead to binding of ATP, activation of the catalytic domain (ATPase activity) and proper orientation of key exposed residues creating a highly specific recognition domain that restricts the phosphoryl transfer to particular substrates. Importantly, other factors may also contribute to regulation of kinase activity, as in the case of Cdk1 where inhibitory phosphorylation of Tyr15 by Wee1 perturbs substrate binding at the catalytic site through steric hindrance. Wee1, along with Cdc25, the PPase relieving the inhibition at Tyr15, constitute the DNA damage checkpoint and delay the cell cycle progression (Ferrari, 2006).

1.2. Phosphatases of *Saccharomyces cerevisiae*

In *Saccharomyces cerevisiae* there are 120 predicted PKs and 32 PPases (Ducruet et al., 2005). This ratio of PKs to PPases is characteristic of eukaryotes and is consistent with high redundancy in PPase function, as well as the use of adaptor proteins for substrate targeting. Budding yeast contains a miniature replica of the larger mammalian PPase network with two major functional families of PPases. The serine/threonine family of PPases is further subdivided into two classes: the phosphoprotein phosphatase P (PPP) family comprised of PP1, PP2A, PP2B subfamilies and the phosphoprotein phosphatase M (PPM) family comprised of the unique PP2C subfamily. The protein tyrosine phosphatase (PTP) family includes the unique subfamily of dual specificity phosphatases (DSP) that can dephosphorylate serine/threonine and tyrosine residues.

A number of PPases found in yeast are highly conserved with orthologs in higher eukaryotes. Examples include *PPH21* and *PPH22* (PP2A orthologs), *GLC7* (PP1

ortholog), *CDC14* (CDC14A/B ortholog) and *MIH1* (CDC25 ortholog). Beyond structural conservation, these PPases also display functional conservation. For example, like its mammalian counterpart, PP2A of *S. cerevisiae* plays a key role in cell cycle regulation and demonstrates similar sensitivity to inhibitors (Haystead et al., 1989; Mumby and Walter, 1993). In contrast, few regulatory subunits associated with these well-documented PPases have clear sequence orthologs in humans (Barford et al., 1998; Bollen, 2001; Carlson, 1999; Ceulemans and Bollen, 2004; Ceulemans et al., 2002), mainly because of the lower complexity of the phosphoproteome in budding yeast. The few regulatory subunits that are well conserved emerged early during evolution and retained similar cellular functions (Barford, 1995; Ceulemans et al., 2002). For example, the mammalian B'γ or B'α regulatory subunits of PP2A can rescue the deletion of *rts1,* the unique B' regulatory subunit ortholog in budding yeast (Zhao et al., 1997).

Glc7, Cdc14, and in some backgrounds Sit4 are essential PPases, suggesting that they function in multiple pathways and/or are essential for cell viability (Sakumoto et al., 2002; Sakumoto et al., 1999). The majority (29/32) of PPases are non-essential and do not yield synthetic lethality in double knockout combinations; in some cases synthetic sickness was observed under specific growth conditions (Sakumoto et al., 2002). This is consistent with the high degree of overlap in the functional network of yeast PPases and suggests high connectivity of the network of interactions among PPases, their regulatory subunits and substrates. Several PPases may be therefore involved in dephosphorylation of a particular substrate at different residues or incomplete dephosphorylation may be sufficient for normal pathway function. An example of this functional overlap is the down-regulation of the yeast MAPK cascades, where six members of the two major PPase families down-regulate cooperatively Fus3 and Hog1 pathways and partially overlap in their regulatory functions (Figure 1-1) (Maeda et al., 1993; Saito and Tatebayashi, 2004; Sakumoto et al., 2002; Wurgler-Murphy et al., 1997;

Zhan and Guan, 1999). This phospho-regulatory model was elucidated through the analysis of synthetic phenotypes from double PPase disruptions, as single mutants did not generate sufficient phenotypic evidence. Additionally, it is possible to speculate that in the absence of the primary interacting PPase the adaptor subunit may recruit another PPase to carry out the hydrolysis of the targeted substrate, further enhancing the functional overlap.

This redundancy makes the analysis of PPase function *in vivo* challenging as it masks genetic and protein-protein interactions by largely buffering null mutations. In the case of the highly conserved PP1 PPase, 14 putative regulatory subunits, thought to provide specificity to particular substrates, have been identified in budding yeast. Over 21 putative regulatory PP1 subunits have been identified in the human genome, suggesting a similar mechanism of PP1 regulation (Ceulemans et al., 2002). However, most experimentally documented regulatory subunits lack clear motifs and appear to have multiple points of contact with the catalytic core (Barford et al., 1998). Thus, in general the structures of adaptor proteins provide little information towards the identification of novel adaptors through sequence analysis alone (Terrak et al., 2004). The high degree of sequence and functional conservation among key cellular PPases combined with similar classification and small proteome size supports budding yeast as a suitable model system for high throughput study of PPase function *in vivo.*

Figure 1-1: Phospho-regulation of the MAPK pathways by PPases

Serine/Threonine (Ptc1, Ptc2 and Ptc3), Tyrosine (Ptp2 and Ptp3) and DSP (Msg5) PPases with distinct substrate preferences dephosphorylate key residues in order to prevent excessive MAPK activation and enable normal growth upon adaptation to the environment. Analysis of double disruptions of *Δmsg5 Δptc2*, *Δmsg5 Δptp2* and *Δptc1 Δptp2* revealed novel synthetic phenotypes undetected in single mutants. These findings contributed to the identification of this regulatory network. (Figure adapted from Saito and Tatebayashi, 2004)

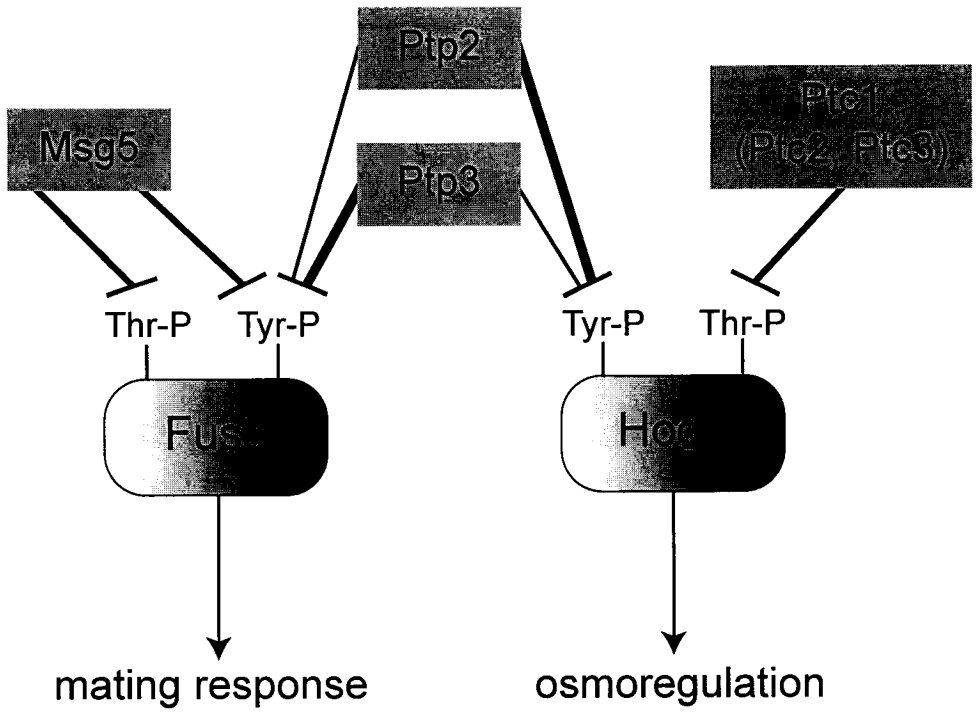
Ptp2
Msg5
Ptp3
Ptc1
(Ptc2, Ptc3)
Thr-P
Tyr-P
Tyr-P
Thr-P
mating response
osmoregulation

Tyrosine specific and dual specificity phosphatases

The expansion of PTPs is closely linked to the development of multicellular organisms and consequently of transmembrane signaling events through receptor protein tyrosine kinases (rPTKs). PTPs are one of the largest PPase families in metazoans with several receptor-like transmembrane proteins and soluble cytosolic proteins. In contrast, budding yeast encodes no authentic rPTKs and only eight cytosolic PTPs, mostly involved in mitogen activated protein kinase (MAPK) signaling (Martin et al., 2005).

All PTPs use a two-step hydrolysis mechanism to remove phosphate groups on tyrosine residues and do not require metal ions (Fauman and Saper, 1996). The homologous catalytic domain with a mean identity of 40% across the family contains the invariant 11 amino acid catalytic motif (I/V)HCXAGXGR(S/T)G (where X is any amino acid), which forms the "P-loop" (Barford, 1995; Barford et al., 1998). The signature motif is situated within the center of the molecule at the base of the catalytic domain and acts as a nucleophile and is essential for catalysis (Romsicki et al., 2003). Firstly, the phosphoryl group of the substrate is transferred to the catalytic site cysteine residue of the P-loop with assistance from an invariant aspartic acid (general acid) located on a mobile loop termed WPD-loop, located ~30 a.a. upstream of the P-loop (Romsicki et al., 2003). Subsequently, the invariant aspartic acid acts as a general base as the phosphate moiety is transferred to a water molecule (Fauman and Saper, 1996; Romsicki et al., 2003). The size and depth of the catalytic pocket of PTPs is thought to limit their activity to the longer and bulkier side chain of tyrosine residues and plays a role in substrate recognition given the preference of PTPs for acidic residues around the phosphorylated tyrosine (Barford, 1995; Fauman and Saper, 1996). One of the key structural features providing this specificity is the phospho-tyrosine recognition loop formed from the conserved sequence KNRY, which defines the depth of the catalytic

pocket and orients the pTyr residue towards the P-loop (Barford, 1995). Evidently, as the structures of the catalytic domains of PTPs are conserved, the functional diversity within the family is generated by the regulatory subunits, which interact with the divergent N and C termini in order to confer substrate specificity to the catalytic subunit.

The DSPs use the same catalytic mechanism as the PTPs, are therefore structurally similar and are classified within the same family. However, DSPs are capable of dephosphorylating residues from all three amino acids mainly due to the absence of the phospho-tyrosine recognition loop (KNRY), which in turn allows for a much shallower and open catalytic site compared to the catalytic pocket of PTPs. This structural difference thus enables DSPs to accommodate the shorter side chains of phospho-serine and phospho-threonine (Zhuo et al., 1994). Over twenty DSPs have been identified in humans and several recognize MAPK as substrates, making them key regulators in growth, differentiation and cell proliferation (Yokota et al., 2006). Budding yeast has five DSPs, which are involved in cell cycle control (Cho et al., 2005) and MAPK pathways (Martin et al., 2005).

Serine/Threonine specific phosphatases

Budding yeast contains 18 serine/threonine PPases forming two major families (PPP and PPM), which can be further divided into four subfamilies. The PPP family consists of eleven PPases classified into three related subfamilies: PP1 (*GLC7, PPZ1, PPZ2, SAL6*), PP2A (*PPH1, PPH21, PPH22, PPH3, PPG1*) and PP2B (*CNA1, CNA2*); and contains one additional unclassified PPase (*PPT1*). The remaining six PPases form the forth subfamily named PP2C and are the unique constituent of the PPM family. Members of the PPM family are divergent structurally from the PPP family and require Mg^{2+} for catalysis. The PPP family accounts for the majority of the protein

serine/threonine PPase activity *in vivo* and contains the highly conserved *PP2A* and *GLC7* PPases, both major regulators in all eukaryotes.

Generally, all members of serine/threonine PPases show poor homology in the non-catalytic N- and C- termini and form a diverse variety of holoenzymes with various regulatory subunits. The catalytic region, however, is highly conserved and all members of the serine/threonine PPase family share the common one step metal-dependent hydrolysis mechanism for the removal of the phosphate group (Holtz et al., 1999; Myles et al., 2001; Terrak et al., 2004). The homology is thus limited to the structurally conserved catalytic pocket, which is shallow and lacks evident substrate specificity. This absence of substrate specificity is in accordance with the requirement for regulatory subunits. (Ceulemans and Bollen, 2004; Egloff et al., 1995; Goldberg et al., 1995). The invariant catalytic phosphoesterase motif $DXH(X)_nG\mathbf{D}XX\mathbf{D}(X)_nGN\mathbf{H}D/E$ (where n~25) relies on a general acid catalyst (histidine) forming a hydrogen bond with carboxyl oxygen of two invariant aspartic acids (Goldberg et al., 1995). The conserved aspartate-histidine pair along with a water molecule, attack the substrate's serine/threonine sidechain, while the other conserved residues provide support and properly orient two metal cations, likely Fe^{2+} and/or Zn^{2}: required to stabilize the negatively charged phosphorylated Ser/Thr residue.

1.3. PP1

Conservation of catalytic and regulatory PP1 subunits

PP1 is one of the most conserved eukaryotic proteins and is a key cellular regulator or "reset switch" with conserved functions in the cell cycle, metabolism, protein synthesis, actin and actomyosin reorganization and finally, ion channels and pumps (Ceulemans and Bollen, 2004; Ceulemans et al., 2002). Bioinformatic analysis of six eukaryotic genomes indicates the early emergence of PP1 in eukaryotes and expansion of its functions with the evolution of the mammalian lineage (Ceulemans et al., 2002). For example, the evolutionary distant fungi *G. lamblia* expresses an isoform of PP1 that is 72% identical to the mammalian PP1 isoforms (Ceulemans and Bollen, 2004). *G. lambalia* separated from eukaryotes shortly after the divergence of archaea and eukaryotes suggesting the early emergence of PP1 as a key cellular regulator. The conserved catalytic subunit of PP1 forms a compact elliptical domain organized into several alpha helices and beta sheets with the catalytic pocket containing the dinuclear metal catalytic site in the center of the molecule (Egloff et al., 1995). The catalytic site lies within the center of a large Y-shaped cleft composed of three branches called the hydrophobic, acidic and C-terminal grooves (Terrak et al., 2004).

Budding yeast *S. cerevisiae* has an unique PP1 ortholog encoded by *GLC7* whereas mammals have three PP1 genes encoding three ubiquitously expressed isoforms: PP1α, PP1γ (two splice variants) and PP1β/δ (Ceulemans and Bollen, 2004). The evolutionary adaptation of PP1 to the expansion of the phospho-proteome was therefore accomplished with the expansion of the number of regulatory subunits. Given that members of the PPP family have on average ~40% of residues in common, the much higher sequence conservation of PP1 across eukaryotes clearly shows that all orthologs adopt nearly identical three-dimensional structure (as is the case for the entire PPP family) and additionally, that residues outside of the catalytic domains are under

selective pressure and thus contribute to the high conservation levels of the primary PP1 amino acid sequence. In fact, the conserved residues outside of the PP1 catalytic pocket are mostly at the surface of the protein and several are located in the Y-shaped cleft, which is postulated to mediate multiple points of contact between PP1 and its regulatory subunits (Ceulemans and Bollen, 2004; Egloff et al., 1997; Terrak et al., 2004). Generally, the numerous protein interactors of PP1 bind through one or more common overlapping binding sites outside of the PP1 catalytic region (Barford et al., 1998). Currently, ~65 genes are known to encode interactors of PP1 in mammals (Ceulemans and Bollen, 2004).

Regulatory subunits of PP1 can be divided into primary and secondary regulators based on whether they originated as regulators of PP1 or acquired PP1 binding function later in evolution. Generally, because of the large binding interface with PP1, all regulatory subunits show low sequence conservation making their identification difficult. Primary regulators contain short PP1 binding motifs and can be identified to some extent by sequence homology. Primary regulators form the more ancient pool of regulatory subunits of PP1, likely part of the initial evolution of PP1 as a key regulator. Secondary regulators, on the other hand, have homologs that do not have PP1 binding sites and appear to have previously performed functions unrelated to PP1, making their evolutionary tracking even more difficult.

Structural studies of primary regulators have identified few binding sites that promote physical interactions with PP1. The most extensively studied motif is the "RVXF" binding channel, which recruits the regulatory subunit to the hydrophobic Y-shaped cleft on PP1. The initial binding of a regulatory subunit through the RVXF motif is thought to act as an anchor. For example the crystallized structure of PP1 with the myosin phosphatase targeting regulatory subunit, myosin-binding phosphatase targeting (MYPT1), shows that the physical interaction occurs over a large intermolecular

interface. The N-terminal part of MYPT1 wraps around PP1 reaching the base of the Y-shaped catalytic cleft and may interact directly with substrates through a steric effect). The middle part of MYPT1 contains the RVXF motif that anchors it to the backside of PP1 and the MYPT1 C-terminus further sustains binding via hydrophobic interactions (Terrak et al., 2004). Binding of MYPT1 has profound effects on the global shape and charge distribution of PP1, producing a holoenzyme with an extended catalytic cleft specifically adapted for myosin substrates and reduced affinity for other substrates (Bollen, 2001; Terrak et al., 2004). Regulatory binding can be sometimes cooperative as the recruitment of the primary regulatory subunit may promote the binding of another regulator further increasing the affinity/specificity for a given substrate. Finally, mutations of key residues within the hydrophobic cleft of PP1 abolish only a subset, rather than all, of the regulatory functions of PP1, demonstrating the complexity of the PP1 regulatory network (Wu and Tatchell, 2001).

Bioinformatic studies have identified large numbers of putative regulatory subunits of PP1 in all metazoans, with orthologs found across all eukaryotes in some cases. Metazoans from flies to humans have multiple genes encoding catalytic subunits of PP1 and possess a wide array of regulatory subunits producing numerous isoforms of PP1 through an assortment of cooperative bindings, rendering research on phospho-regulatory roles of PP1 very complex. Budding yeast, on the other hand has nine experimentally confirmed regulatory subunits, enormously simplifying the understanding of key roles of PP1 in biological processes conserved among eukaryotes.

Biological functions of Glc7

Similar to the multiple isoforms of PP1 in higher eukaryotes, Glc7 is a master regulatory switch in yeast and localizes to multiple subcellular compartments in a cell cycle dependent manner (Figure 1-2A and B) (Bloecher and Tatchell, 2000). The single PP1 ortholog in yeast (Glc7) was initially characterized in budding yeast as one of the "glc" genes responsible for defects in glycogen accumulation (Feng et al., 1991). To date, Glc7 has nine established regulatory subunits (Gac1, Reg1, Reg2, Ref2, Sip5, Glc8, Bud14, Bni4 and Sds22) and plays important regulatory roles in glycogen metabolism, sporulation, mitosis, mRNA export and osmoregulation.

Glc7 promotes the transition to more efficient energy sources when carbon sources are abundant and promotes the storage of energy in the form of glycogen (Ceulemans and Bollen, 2004) by binding to a subset of known regulatory units involved in glucose metabolism and glycogen synthesis, mainly Gac1, Reg1, Glc8 and Gip2 (Dombek et al., 1999; Nigavekar et al., 2002; Williams-Hart et al., 2002; Wu et al., 2001; Wu and Tatchell, 2001). The metabolic shift caused by nutrient starvation involves direct modification of metabolic pathways and affects expression of ~40% of the 6,200 genes of *S. cerevisiae*. These changes are orchestrated in part by conserved trimeric PKs, which are downstream effectors of the Ras/cAMP/PKA pathway (Ceulemans and Bollen, 2004; Santangelo, 2006). These serine/threonine PKs termed Snf1 in yeast and AMP-activated kinase (AMPK) in higher eukaryotes share a common regulatory mechanism based on reversible phosphorylation (Carlson, 1999). Snf1 of budding yeast acts as a positive regulator of gluconeogenic pathways (Carlson, 1999) and upregulates glucose import, gluconeogenesis, respiration and use of alternate carbon sources through direct phosphorylation and transcriptional means. The inhibitory dephosphorylation of Snf1 by Glc7 complexed with the RVXF containing regulatory subunit Reg1 and Sip5 reestablishes glucose as the preferred source of energy and reinitiates anabolic

glycolysis pathways (Ceulemans and Bollen, 2004). *glc7* alleles structurally defective in recruiting Reg1 show defects in glucose repression and maintain high levels of active Snf1 (Tu and Carlson, 1995) and can be rescued by over-expression of *REG1* (Santangelo, 2006; Tu and Carlson, 1995). As PP1/Glc7 is also a histone H3 phosphatase (Hsu et al., 2000), it may also control glucose repression through direct dephosphorylation of Snf1 targets. Known *glc7* alleles impaired in their interactions with the regulatory subunit Gac1 are defective in glycogen accumulation. The Gac1-Glc7 complex primarily regulates glycogen accumulation by activating Gsy1 and Gsy2 through dephosphorylation of three residues near the C-terminus of these two glycogen synthases (Guillou et al., 2004). These two proteins are 80% identical and share about 50% identity with the mammalian muscle and rat liver glycogen synthase. Deletion of Gsy2, the predominant glycogen synthase, results in a 90% decrease in glycogen content (Francois and Parrou, 2001). Similarly, the loss of glycogen associated PP1-G_M complex in rat hepatocytes has been associated with impaired glucose-induced activation of glycogen synthase as seen in insulin-dependent diabetes (Ceulemans and Bollen, 2004).

A subset of known *glc7* alleles show increased rates of chromosome loss, indicating their inability to properly orchestrate the segregation of the genetic material during mitosis. Moreover, conditional *glc7* alleles show a clear G2/M delay and arrest at non-permissive temperatures as large budded cells with a 2N DNA content (Bloecher and Tatchell, 1999). Glc7 dephosphorylates substrates of the Ipl1 aurora B kinase, an important regulator of kinetochore attachment and the spindle assembly checkpoint, most likely through its association with the Sds22 regulatory subunit (Peggie et al., 2002). Interestingly, Sds22 is the only known essential PP1 subunit in budding yeast and lacks the RVXF binding motif (Peggie et al., 2002). Most *glc7* alleles sporulate poorly, indicating deficiencies in DNA duplication, segregation and spore packaging. Glc7-Red1

and Glc7-Gip1 complexes are thought to control the first meiotic chromosomal division and spore wall synthesis/spore packaging respectively (Ramaswamy et al., 1998). Mammalian PP1 has retained similar functions since it is targeted to multiple mitotic structures and microinjection of PP1-antibodies in cultured mammalian cells results in mitotic arrest (Andreassen et al., 1998).

Glc7 localizes to sites of polarized growth (bud tip, bud cortex and bud neck) and may stabilize microtubule interactions at these locations (Figure 1-2A) (Bloecher and Tatchell, 2000; Knaus et al., 2005). Randomization of the bud site selection, morphological abnormalities, loss of the actin ring at the bud neck and microtubule (MT) dependent events such as nuclear migration and spindle orientation are defective in some *glc7* mutants (Andrews and Stark, 2000; Bloecher and Tatchell, 2000; Cullen and Sprague, 2002). The recruitment of Glc7 to these locations requires formation of Glc7-Bud14 and Glc7-Bni4 complexes (Kozubowski et al., 2003; Pinsky et al., 2006). The regulatory subunit Bud14 interacts genetically with *KAR3*, *KAR9* and *BIM1*, involved in MT-dependent nuclear migration. The regulatory subunit Bni4 interacts physically with Cdc10, one of the five components of the septins (Cdc3, Cdc10, Cdc11, Cdc12, and Shs1/Sep7) (Gladfelter et al., 2001). The septin containing cortex is thought to act as a scaffold, recruiting many other proteins to the bud neck, where they can perform various functions required for proper cytokinesis, morphogenesis and cell wall deposition (Longtine et al., 1996). Additionally, Bni4 interacts genetically with Mbs2 a component of the Cdc42 signaling pathway required for formation of the septin ring, possibly in part through activation of Cla4 (Cullen et al., 2004). Cla4, a p21-activated kinase, phosphorylates certain septins and the absence of Cla4 causes aberrant septin organization (Versele and Thorner, 2004). It is conceivable that Glc7 may antagonize Cla4 or play a role in its Cdc42-dependent activation. Regulatory subunits of mammalian

PP1 holoenzymes acting on the actin cytoskeleton are far more numerous and are principally expressed in neural and muscle tissues (Ceulemans and Bollen, 2004).

Figure 1-2: Glc7-GFP localization in living cells

Wild-type cells expressing endogenous levels of Glc7-GFP were imaged with a spinning disk confocal microscope (0.5 µm optical sections) as described in (Cuschieri et al., 2006). **(A)** Glc7-GFP localizes to sites of polarized growth during bud emergence and bud growth (bud cortex and bud tip), the bud neck and the nucleus. Prior to anaphase, Glc7-GFP is detected in the nucleolus. **(B)** During cytokinesis, Glc7-GFP is detected in the nucleus, and accumulates at the spindle poles and the site of cytokinesis (abcission; 09:29). (Figure by Michael Logan)

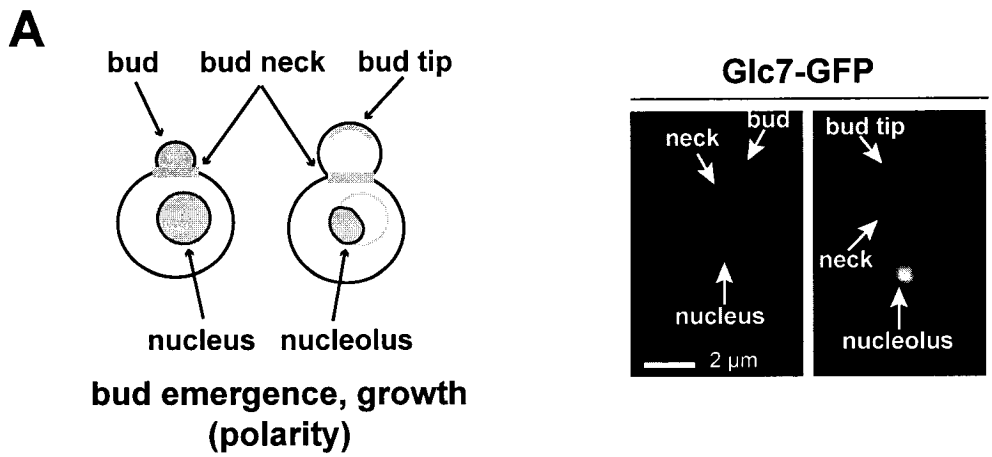
A
bud
bud neck
bud tip
nucleus
nucleolus
bud emergence, growth
(polarity)
Glc7-GFP
neck
bud
bud tip
neck
nucleus
nucleolus
2 µm
B
SPBs
cytokinetic ring
nucleus
cytokinesis (anaphase)
Glc7-GFP
nucleus
SPB
SPB
CR
2 µm
Glc7-GFP
Time-lapse (min:sec)
00:00
00:29
00:59
01:29
01:59
02:29
02:59
03:29
03:59
04:29
04:59
05:29
05:59
06:29
06:59
07:29
07:59
08:29
08:59
09:29

In addition, the nuclear Glc7 holoenzyme is involved in modulating mRNA export through phospho-regulation of mRNA-protein (mRNP) complexes. The dephosphorylated complexes are recruited to the nuclear pore complex and transit to the cytoplasm where they dissociate from the mRNA upon phosphorylation by Sky1 (Gilbert and Guthrie, 2004). Glc7 also contributes to recovery from starvation/stress by opposing the Gcn2 protein kinase that phosphorylates the α subunit of the translation initiation factor eIF2, a key step required for activation of the translation initiation factor Gcn4 (Wek et al., 1992). Gcn4 controls the general amino acid control mechanism that regulates the transcription of several amino acid biosynthetic genes, representing 12 different pathways, in response to starvation and may ultimately induce the transcription of up to a thousand genes in budding yeast (Hinnebusch and Natarajan, 2002). Finally, Glc7 also plays a role in homeostasis as some alleles are sensitive to cations and alkaline pH, but not to sorbitol indicating defects in ion transport despite normal osmoregulation (Williams-Hart et al., 2002).

Overlapping functions have also been demonstrated for Glc7 regulatory subunits. For example, Glc8 is a regulatory subunit of Glc7 which plays an established role in chromosome segregation and sporulation (meiosis), but was initially identified along with Glc7 as a much milder glycogen deficient mutant (Cannon et al., 1994). Another interesting example is Sds22. While Sds22 is involved in chromosome stability and mitosis it also interacts physically with Reg1, Snf4 and Snf1 (Graumann et al., 2004; Ho et al., 2002). The latter two proteins are components of the trimeric AMP-activated kinase regulating gluconeogenic pathways thus linking mitotic events (Glc7-Sds22) with metabolism (Glc7-Reg1).

The emerging picture for Glc7 is one of a multimeric enzyme with multiple isoforms executing pleiotropic and overlapping functions. Glc7-dependent phospho-regulation is complex and remains vastly unexplored with 95 known physical interactions

catalogued in the BIND database, but very few genetic interactions recorded in the SGD and BIOGRID databases (~20). This situation requires the development of novel tools for proteomic and genomic studies adapted to investigate the phospho-regulatory network of Glc7.

1.4. Thesis proposal

While PK function has been studied intensively in budding yeast (Bishop et al., 2001; Zhu et al., 2001) the analysis of PPase function has lagged due to the high redundancy of the PPase interaction network, which in turn masks genetic and physical interactions. Therefore, a lot of PPase-dependent defects are not detected in genetic screens. Moreover, selecting the right combination of double mutants (i.e. double PPase mutants or the combined mutation of a PPase and a regulatory subunit) that will yield scorable phenotypes is challenging given the small pool of studies done on phosphatases and the functional overlap between regulatory subunits.

Previous studies have used either knockout mutations or point mutations that lie outside the catalytic domain of the core PPase subunit. These studies, in particular those utilizing point mutations, yielded regulatory subunits and functions for PPases. This has been a particularly useful approach for PP1/Glc7 (Anderson and Tatchell, 2001; Baker et al., 1997; Bloecher and Tatchell, 2000; Sakumoto et al., 2002; Sakumoto et al., 1999). However, both approaches are limiting for the following reasons. Studies employing catalytic subunit knockout mutations have demonstrated the high functional overlap present within the yeast PPase network (Sakumoto et al., 2002). Functionally redundant PPases will partially compensate for a knockout mutation, and thereby mask genetic interactions. Furthermore, the absence of the catalytic subunit using the knock-out senario prevents the direct identification of interaction partners and substrates. Thus, any large-scale analysis directed at uncovering specific genetic interactions through this

method would be not be expected to reveal substrates and likely to have a high number of false negatives, resulting in a poorly defined (e.g. pathways versus substrates) and incomplete genetic interaction dataset. The second set of studies relied on point mutations outside the catalytic subunit, either distorting the overall tertiary confirmation of the protein or affecting the regulatory units binding regions. These studies have yielded valuable function-specific data sets (Andrews and Stark, 2000; Baker et al., 1997; Cannon et al., 1994; Ramaswamy et al., 1998). However, the potential for such mutants to be separation of function alleles limits their usefulness in large-scale analyses intended to interrogate a broad spectrum of Glc7 function *in vivo*.

We hypothesize that the use of a hypomorphic catalytic mutant, which is structurally intact and thus conserves normal stochiometry and holoenzyme structure, will uncover a wider and more complete set of interactions between the catalytic core, its regulatory subunits and substrates. By maintaining wild-type PPase to substrate(s) ratio(s) within its phospho-regulatory network, the catalytic PPase mutant should shield its substrates from other PPases and as a result reduce, and perhaps even eliminate, the problem of functional redundancy among PPases. The systematic mutagenesis of protein PPases into catalytically compromised mutants in *Saccharomyces cerevisiae* is thus a novel approach for global analysis of PPase function *in vivo* and will circumvent some of the previous experimental limitations. My research project focuses on a novel hypomorphic allele of Glc7 suitable for high-content genetic and proteomic screens that will lead to the creation of a network of interactions between Glc7, its regulatory subunits and substrates, thus ultimately improving the knowledge of the phospho-regulatory mechanism of the cell and its impact on vital cellular functions.

Chapter 2: Analysis of yeast PP1/Glc7 phosphatase functional networks using an integrated genomic and proteomic approach

2.1. Introduction

Regulation of phosphorylation state is a mechanism for controlling the function, localization and stability of proteins in vivo and is critical for the regulation of essential processes such as polarity and morphogenesis, chromosome segregation, cytokinesis, and cell cycle control (Andrews and Stark, 2000; Dobbelaere et al., 2003; Pinsky et al., 2006; Stegmeier and Amon, 2004). Together, protein kinases (which mediate phosphorylation) and protein phosphatases (PPases) (which mediate de-phosphorylation) provide precise temporal and spatial regulation of their target substrates. In the yeast *Saccharomyces cerevisiae*, the dynamic localization of PPases suggests that an extensive cross talk between these processes is critical for the proper execution of cell division (Bloecher and Tatchell, 2000; Dobbelaere et al., 2003). However, many of the substrates and regulatory proteins that participate in this cross talk remain unidentified. Insight into PPase function has lagged significantly in comparison to kinases since PPases: (1) frequently require regulatory proteins that dictate the specificity of the PPase to a particular substrate, location or process and (2) exhibit considerable functional redundancy; of the 32 PPases in budding yeast ~90% are non-essential (Sakumoto et al., 2002).

To date, investigations of PPase function in budding yeast have utilized either mutations outside the catalytic site (Bloecher and Tatchell, 2000; Terrak et al., 2004; Wu et al., 2001; Wu and Tatchell, 2001) or probed genetic interactions using single or double knockout PPase mutations (Sakumoto et al., 2002). These approaches present constraints for large-scale analysis of PPase function for several reasons: (1) mutations outside the catalytic domain generally affect the formation of a specific class of

holoenzyme or the ability to interact with co-factor(s) required for the proper targeting of the PPase to a subset of substrates (Ceulemans and Bollen, 2004; Knaus et al., 2005; Ramaswamy et al., 1998), (2) the use of knockout alleles may lead to promiscuous and/or low-affinity interaction of regulatory subunits with PPases of the same class and, thereby, preclude the analysis of the essential PPases, and (3) functional redundancy and compensation between different PPase classes (Sakumoto et al., 2002) strongly suggests that no single method of analysis will uncover regulatory subunits, substrates and functional networks for a given PPase. For these reasons, we designed a strategy based on a hypomorphic catalytic PPase mutation that uses two complementary large-scale approaches; the Synthetic Genetic Array (SGA) and 2D difference gel electrophoresis (2D-DiGE). High throughput generation of a large number of double mutant combinations (by SGA) has been successfully used to examine genetic interaction networks in yeast in a wide range of cellular processes (Davierwala et al., 2005; Drees et al., 2005; Tong et al., 2001; Tong et al., 2004). Post-translational modifications and changes in relative abundance at the proteome level can be identified using the 2D-DiGE method (Unlu et al., 1997). We anticipated a comparison of datasets obtained from the analysis of genetic interactions using the SGA and of changes in the proteome using 2D-DiGE would help in assessing whether a genetic interaction or change in protein abundance or modification has biological significance.

In the budding yeast Saccharomyces cerevisiae, 32 genes encode predicted or demonstrated catalytic subunits of PPases. Only two of these PPases are clearly essential; the PP1-type PPase, Glc7 (GLyCogen deficient strain) (Andrews and Stark, 2000; Baker et al., 1997), and Cdc14 (cell division cycle), a dual-specificity phosphatase that plays a central role in the MEN pathway controlling mitotic/meiotic exit (Wan et al., 1992). We selected Glc7 for our analyses as it has been extensively characterized by analysis of conditional mutants, but had not been subjected to large-scale genetic or

proteomic analyses. Glc7 critically regulates numerous processes such as glucose and glycogen metabolism, sporulation, chromosome segregation, meiosis, mRNA transport, transcription, and amino acid biosynthesis (Andrews and Stark, 2000; Baker et al., 1997; Ceulemans and Bollen, 2004; Pinsky et al., 2006; Sanz et al., 2000a; Tu and Carlson, 1995; Wu et al., 2001). To date, Glc7 has been shown to physically interact with 95 different proteins (BIND database). Some of these proteins are known substrates (Cbf2, Fin1, Red1, Gsy2), while others are thought to be regulatory subunits (Gac1, Reg1, Reg2, Ref2, Sip5, Glc8, Bud14, Bni4, Sds22). However, the functional significance of the majority of these interactions remains unclear. Relatively few (26) genetic interactions have been described for glc7 mutants (BioGRID), many of which are dosage dependent. The functional clustering of genetic interactions of conditional glc7 alleles suggest the majority these mutations compromise a specific aspect of Glc7 function. As such, these alleles are highly suited for cell biology but may be less suited for large-scale analyses directed a revealing a comprehensive picture of Glc7 signaling in vivo.

In an effort to further define the signaling network for Glc7, we created a novel *glc7* catalytic mutant (*glc7-E101Q*) suitable for both SGA and 2D-DiGE analysis. The *glc7-E101Q* mutant exhibited slow growth and impaired glycogen accumulation on glucose, but no specific delay in the cell cycle. The impaired growth and defects in glycogen synthesis of the *glc7-E101Q* mutant were rescued by introduction of a single copy of wild-type *GLC7*, indicating that *glc7-E101Q* is a recessive, hypomorphic allele. SGA analysis revealed a broad network of synthetic genetic interactions (147 synthetic sick/lethal (SSL) and 178 synthetic rescue (SR)) that encompass all of the known Glc7-regulated processes, and suggesting additional previously unknown functions. Parallel analysis of SGA and 2D-DiGE data identified a non-essential enolase (Eno1) as both a genetic suppressor of *glc7-E101Q* and a mis-regulated protein in *glc7-E101Q* cells. The *glc7-E101Q eno1Δ* double mutant showed improved spore viability relative to *glc7-*

E101Q, but retained glycogen accumulation defects. Our findings suggest a role for Eno1 in the regulation of spore survival. Together, our results demonstrate that the use of complementary approaches such as SGA and 2D-DiGE can facilitate the identification of interaction partners.

2.2. Materials and Methods

2.2.1. Media, growth conditions and strain manipulations

Yeast strains (Table 1) were created through PCR-based transformation (Christianson et al., 1992; Longtine et al., 1998). Media (rich media; YPAD (2% glucose), YPAG (3% glycerol with 0.08% glucose) and synthetic complete, SC) were prepared as previously described. Standard methods for culture of yeast strains and integrative transformation, mating, sporulation and tetrad analysis was performed as previously described (Guthrie, 1991). SGA analysis and *glc7-E101Q eno1*Δ interaction analyses were performed in strains derived from the s288c diploid BY4743 (Brachmann et al., 1998), all other analyses were performed in strains derived from the s288c diploid Y270 (Vogel et al., 2001).

Table 2-1: Yeast strains used in this study

Strain	Genotype	Source
BY4743	*MATa/α ura3Δ0/ura3Δ0 leu2Δ0/leu2Δ0 his3Δ1/ his3Δ1 LYS2/lys2-Δ0 met15Δ0/MET15*	(Brachmann et al., 1998)
Y270	*MATa/MATα ura3Δ-52/ura3Δ-52 lys2Δ-801/lys2Δ-801 ade2Δ-101/ade2Δ-101 trp1Δ-901/trp1Δ -901 his3Δ-200/his3Δ-200*	(Vogel et al., 2001)
Y5563	*can1Δ::MFA1pr-HIS3 lyp1Δ his3D1 leu2Δ0 ura3Δ0 met15Δ0*	H Bussey, C Boone
ΔArrayORF	*MATa orfΔ*::KanMX6 *LYS2 his3Δ1 leu2Δ0 met15Δ0 ura3ΔO*	(Winzeler et al., 1999)
YNS3	*MATa ura3Δ-52 lys2Δ-801 ade2Δ-101 trp1Δ-901 his3Δ-200*	This study
YNS2	*MATα ura3Δ-52 lys2Δ-801 ade2Δ-101 trp1Δ-901 his3Δ-200*	This study
YNS19	*MATa/MATα glc7-D91N:KanMX6/GLC7 ura3Δ-52/ura3Δ-52 lys2Δ-801/lys2Δ-801 ade2Δ-101/ade2Δ-101 trp1Δ-901/trp1Δ -901 his3Δ-200/his3Δ-200*	This study
YNS23	*MATa GLC7:ProA:KanMX6 ura3Δ-52 lys2Δ-801 ade2Δ-101 trp1Δ-901 his3Δ-200*	This study
YNS26	*MATα glc7-E101Q:ProA:KanMX6 ura3Δ-52 lys2Δ-801 ade2Δ-101 trp1Δ-901 his3Δ-200*	This study
YNS27	*MATa glc7-E101Q:ProA:KanMX6 ura3Δ-52 lys2Δ-801 ade2Δ-101 trp1Δ-901 his3Δ-200*	This study
YNS44	*MATα GLC7:ProA:KanMX6 ura3Δ-52 lys2Δ-801 ade2Δ-101 trp1Δ-901 his3Δ-200*	This study
YNS53	*MATa/MATα glc7-E101Q:KanMX6/GLC7 ura3Δ-52/ura3Δ-52 lys2Δ-801/lys2Δ-801 ade2Δ-101/ade2Δ-101 trp1Δ-901/trp1Δ -901 his3Δ-200/his3Δ-200*	This study
YNS90	*MATα glc7-E101Q:kanMX6 ura3Δ-52 lys2Δ-801 ade2Δ-101 trp1Δ-901 his3Δ-200*	This study
YNS91	*MATa glc7-E101Q:KanMX6 ura3Δ-52 lys2Δ-801 ade2Δ-101 trp1Δ-901 his3Δ-200*	This study
YNS98	*MATα glc7-E101Q:NatMX4 can1Δ::MFA1pr-HIS3 lyp1Δhis3D1 leu2Δ0 ura3Δ0 met15Δ0*	This study
YNS128	*MATa/MATα glc7-E101Q:KanMX6/GLC7 ura3Δ-52/ ura3Δ::GLC7:URA3 lys2Δ-801/lys2Δ-801 ade2Δ-101/ade2Δ-101 trp1Δ-901/trp1Δ -901 his3Δ-200/his3Δ-200*	This study
YNS138	*MATa glc7-E101Q:KanMX6 ura3Δ::GLC7::URA3 lys2Δ-801 ade2Δ-101 trp1Δ-901 his3Δ-200*	This study
YNS141	*MATα glc7-E101Q:KanMX6 ura3Δ::GLC7::URA3 lys2Δ-801 ade2Δ-101 trp1Δ-901 his3Δ-200*	This study

2.2.2. Mutagenesis of Glc7 and strain construction

A 1.2 kb PCR product containing 3' sequence of the *GLC7* ORF was cloned into pBSK using *KpnI* and *NotI* to create pGLC7-1. The *kanMX6* selection cassette was amplified by PCR from pFA6A-kanMX6, digested with *NotI* and *SacI* and cloned into pGLC7-1, creating pGLC7-kanMX6. This construct was used as a template for PCR-based mutagenesis of the catalytic domain at codon 273 (D91N: GAT to AAT) and codon 303 (E101Q: GAG to CAG). A silent restriction site (*AvrII* in D91N and *HindIII* in E101Q) was introduced into the mutagenic 5' primer to mark the mutation. Mutagenic PCR products were transformed into an s288c diploid strain (Y270) as previously described (Vogel *et al.,* 2001), and Kan-resistant transformants selected for on YPAD containing 200 µg/ml G418 (GIBCO). Integration into the *GLC7* locus was confirmed by amplification of a PCR product that spanned the ORF and the KanMX6 cassette and by restriction digest with *AvrII* or *HindIII*. Finally, the presence of a single point mutation (D91N or E101Q) in the ORF and no others was confirmed by sequencing. Diploid strains heterozygous for D91N (YNS19) and E101Q (YNS53) mutations were sporulated, and haploid *glc7-E101Q:KanMX6* MATa and MATa segregants (YNS91, YNS90) isolated for phenotypic, growth and 2D-DiGE analyses. A similar cloning strategy was used to create ProA fusions of both wild-type *GLC7* and *glc7-E101Q*. A Glc7 PCR product lacking the endogenous stop codon was cloned into pBSK (pGLC7-2) and the ProA and KanMX6 selectable markers from pFA6A-ProA-kanMX6 (Knop et al., 1999) integrated using *NotI* and *SacI,* creating pGLC7-ProA. This construct was used for PCR directed mutagenesis and transformation into Y270 as described above, sporulated and haploid segregants (YNS26, YNS27) isolated for the analysis of protein stability. Wild-type GLC7-proA strains were derived in a similar manner (YNS23, YNS44).

For *glc7-E101Q* rescue experiments, a *GLC7* was cloned into the integrative plasmid pRS306 by first amplifying a PCR product from genomic DNA that contained the entire

GLC7 ORF and 0.5 kb 5' promoter sequence and 0.3 kb 3' UTR, digested with *KpnI* and *SacI* and ligated into pRS306 (Sikorski and Hieter, 1989), resulting in pGLC7-3. pGLC7-3 was linearized with *StuI*, and transformed into the *ura3* locus of the heterozygous diploid strain YNS53. Integration at the *ura3* locus resulted in wild-type copy of *GLC7* marked with *URA3* (YNS138, YNS141; *GLC7-res*) on the opposite arm (116167-116970) of chromosome V relative to the *GLC7* locus (432491-433954). In ~40 meiotic events *GLC7-res* segregated as an un-linked gene (28TT : 3NPD : 9PD) independently of *GLC7* and *glc7-E101Q*.

To create the SGA query strain, YNS98, a *NatMX4* PCR product with homology to the *GLC7* 3' UTR sequences was amplified by PCR from p4339 (Tong et al., 2001), and used to replace the KanMX cassette in YNS90. Genomic DNA of the resulting strain was then used to amplify a PCR product containing the E101Q mutation and the NatMX4 cassette. This PCR product was transformed into Y5563 according to previously described methods (Tong et al., 2004).

2.2.3. Growth assays, FACS and glycogen staining

To determine cell doubling time, wild-type (YNS2, YNS3) and *glc7-E101Q* (YNS90, YNS91) strains were grown to mid-log phase in YPAD, diluted to 0.1 OD units and incubated at 30˚C for 3 hours to re-initiate early log phase growth. Cells were collected at 60 minute intervals for 4 hours, and cell density determined using a hemocytometer, with the cell density at time=0 normalized to 1.0. The average doubling time (minutes) was calculated from the slope (R^2>0.95) of the change in cell density (log) relative to time. Budding index was determined by counting the proportion of un-budded, small-budded (bud <50% mother cell) and large-budded cells in wild-type and mutant strains. Cells were pre-treated with Zymolase (20 µg/ml) to complete cell separation. For spotting assays, log phase cells grown in liquid YPAD were diluted, and ~3000 cells (~20 µl/spot) spotted to YPAD or YPAG plates and incubated for 2-3 days at 30°C. Glycogen content was determined as previously described (Enjalbert et al., 2000) Briefly, after incubation for 2 days at 30˚C plates were exposed to iodine crystals (Sigma) for 1 minute, removed for 15 sec and exposed again for 2 min. Digital images were captured immediately after exposure to iodine. Cell cycle progression of wild-type and *glc7-E101Q* strains was determined by FACs analysis as previously described (Dien et al., 1994).

2.2.4. Synthetic Genetic Array (SGA) analysis of *glc7-E101Q*

SGA analysis was performed using the ordered deletion array and Virtek pinning robot system as previously described (Tong et al., 2001; Tong et al., 2004; Winzeler et al., 1999). The sizes of the resulting colonies were measured from digital images of the plates. A comparative set of mutant measurements relative to wild-type control measurements enabled t-statistics and p-values to be calculated (Tong et al., 2004). Double mutants that showed significantly reduced or enlarged colony sizes ($p<0.05$)

were scored as synthetic sick/lethal (SSL) or synthetic rescue (SR), respectively. *GLC7* is an essential gene known to function is a broad spectrum of processes, thus it was anticipated that a large number of *glc7-E101Q* genetic interactions would be identified using SGA. This proved to be the case, as >300 SSL interactions were identified in the initial SGA analysis. Also, we wished to obtain the most comprehensive dataset of interactions and minimize the number of false negatives; this dataset could subsequently be re-screened when an automated random spore analysis protocol became available (the secondary random spore confirmation of >500 SSL and SR interactions began in April 2007). For these reasons, and in contrast with the majority of previously published SGA datasets derived from non-essential genes used as query alleles, the *glc7-E101Q* SGA analyses were performed twice (each in triplicate) and the second analysis used for confirmation of the first. The overlap for the two screens was 60% for SSL and 39% for SR interactions, and is consistent with results for random spore confirmations of two recent SGA screens performed by the Vogel group. Both screens used point mutations in the essential genes *TUB4* and *AME1* as query alleles and as with *glc7-E101Q*, revealed a large number of interactions (unpublished data, T. Nguyen and J Vogel). It should be noted that the final *glc7-E101Q* interaction dataset used for publication will consist of interactions confirmed by random spore and/or tetrad analysis.

2.2.5. Protein extraction, 1D and 2D-SDS-PAGE and 2D-DiGE analysis

All steps were performed at 4°C unless otherwise indicated. Log phase yeast cultures were harvested and washed in PGSK+ buffer (PGSK+: 50 mM NaPO4, 50 mM NaCl, 5 mM KCl, 60 mM glucose, 4% CHAPS, 50mM DTT, 5 µM yeast protease inhibitors [Sigma P8215], 5 µM PMSF, 5 µM ortho-vanadate, 5 µM NaF, and 5 mM β-glycerol phosphate) and pelleted by centrifugation. Cell pellets were suspended in 2 volumes of PGSK+, and an equal volume of zirconium beads (Biospec Products) added,

and cells lysed by 10 cycles of vortexing (1 min) and incubation (1 min) on ice. Extracts were cleared by centrifugation for 10 min at 13,000 x g. For 1D SDS-PAGE, extracts were re-suspended in an equal volume of 2X SDS sample buffer (Laemmli, 1970) and denatured at 95°C for 5 min. For 2D-DiGE, extracts were treated with 50 µg/ml DNAse and RNAse (Worthington) for 15 minutes, acetone-precipitated and re-suspended in labeling buffer (2M thiourea, 7M urea, 6mM DTT, 4% CHAPS) at 25°C and the protein concentration of the samples determined (Biorad Protein Assay). For 2D-DiGE analyses, paired samples (50 µg each) were labeled with NHS-Cy dyes (Cy3 and Cy5, respectively) according to the standard minimal labeling protocol (Unlu et al., 1997). A pooled sample composed of equal amounts of all extracts labeled with Cy2 (50 µg) was co-loaded as an internal standard (total 150 µg/IPG strip) (Table 2-2). Strip rehydration and isoelectric focusing for 2D-DiGE analyses was performed using 13 cm pH 3-11 NL IPG strips (GE), according to the manufacturer's instructions. Focused proteins in IPG strips were resolved using 11% Ruby SDS-PAGE gels (GE). All 2D-DiGE experiments were performed in triplicate using reciprocal labeling (see results), and gel images collected at 100 µm resolution using a Typhoon 9400 trio+ scanner and Image-Quant software. A spot list was generated using DeCyder v6.5 (BVA Module). Significant changes in protein abundance between the four conditions analyzed was performed using 2-way ANOVA (Decyder Software v6.5).

Table 2-2: 2D-DiGE: experimental design using the pooled internal standard

Gel	Cy2	Cy3	Cy5	Comment
1	Pooled Standard	*glc7-E101Q* (dextrose)	WT (dextrose)	Fermentation Biological replicate #1
2	Pooled Standard	WT (dextrose)	*glc7-E101Q* (dextrose)	Fermentation Biological replicate #2 Cy dye reversal
3	Pooled Standard	*glc7-E101Q* (dextrose)	WT (dextrose)	Fermentation Biological replicate #3
4	Pooled Standard	*glc7-E101Q* (glycerol)	WT (glycerol)	Respiration Biological replicate #1
5	Pooled Standard	WT (glycerol)	*glc7-E101Q* (glycerol)	Respiration Biological replicate #2 Cy dye reversal
6	Pooled Standard	*glc7-E101Q* (glycerol)	WT (glycerol)	Respiration Biological replicate #3

2.2.6. Immunoblotting

Immunoblotting was performed as previously described (Vogel et al., 2001). Briefly, proteins extracts prepared from *GLC7:ProA:kanMX* (YNS23, YNS44) and *glc7-E101Q:ProA:kanMX* (YNS26, YNS27) strains were separated on 10% SDS-PAGE gels, transferred to PVDF membranes (Millipore) and probed with anti-ProA monoclonal antibodies (1:5000; clone SPA-27, Sigma). Actin was detected using the monoclonal antibodies (1:5000; clone C4, MP Biomedical). Protein/antibody complexes were detected using anti-mouse HRP-conjugated secondary antibodies (1:10,000; GE HealthCare) and ECL chemi-luminescence (Pierce).

2.2.7. LC-MS/MS (QTRAP)

Spots were excised from deep purple gels counter-stained with silver, digested with trypsin and tryptic peptides analyzed on a QTrap 4000 linear ion trap mass spectrometer (Sciex-Applied Biosystems, Concord, Ont). A peak list was generated using BioAnalyst 1.4 software (Applied Biosystems) and submitted to Mascot (Matrix Science) for peptide identification using the NCBI database as a source. Significant molecular weight search (MOWSE) scores ($p<0.05$) along with protein coverage were used to identify Eno1.

2.3. Results

glc7-E101Q is a hypomorphic GLC7 catalytic allele

Glc7 is the sole essential member of the PPP family of PPases in budding yeast. Members of the PPP family share a conserved catalytic motif. Residues in the Glc7 catalytic domain (CD1, CD2 and CD3) are evolutionarily conserved with human PP1 orthologs and the PP1-like bacterial λ-PPASE (Figure 2-1A). The three-dimensional structure of human PP1 (PP1C-γ; PDB Model 1jk7A), which shares 87% identity and 94% similarity with Glc7, was used as a template for homology modeling of the catalytic domain of Glc7 (aa7-297) using PDBViewer (v.3.9b1) (Guex and Peitsch, 1997). The resulting 3D model (score of 562 bits (1448), expected = e-161) is shown in Figure 2-1B (left panel).

The threaded structure of Glc7 forms a compact elliptical domain composed of alpha-helices and beta-sheets, the core of the structure is composed of a pair of mixed beta-sheets (Egloff et al., 1995; Egloff et al., 1997). Glc7 has a shallow catalytic pocket with no evident substrate specificity, which is in accordance with the broad substrate specificity of its PP1 homologues. Moreover, the conserved metal ion-coordinating residues and catalytic residues in CD1, CD2 and CD3 are also mainly located on the intervening loops and cluster in the tertiary structure to form the catalytic pocket of Glc7 (yellow residues; H124, D91, D94 shown in green) that is very similar to that of human PP1 (PP1C-γ: blue and Glc7 aa7-297: pink) (Barton et al., 1994)). The N-terminus is not highly conserved (Egloff et al., 1997) and therefore the first 6 amino acids of Glc7 could not be threaded. The rest of the N-Terminus folds into a hydrophobic alpha-helix tucked against the surface of the molecule. The C-terminus folds into a hydrophilic alpha-helix that appears to be exposed, protruding away from the core of the structure. The last ~15 amino acids are not conserved, show a high probability of a disordered region based on

PSIPRED (McGuffin et al., 2000) (Appendix, Figure S1), and were therefore not threaded.

Given the high degree of conservation in the catalytic residues, Glc7 is expected to have catalytic characteristics similar to those of previously characterized PP1-type PPases. Phosphate hydrolysis by PP1 occurs via a one-step reaction, and is dependent on a metal ion catalyst (Zn^{2+}, Fe^{2+} or Mn^{2+}). This hydrolysis reaction is dependent on a phosphoesterase motif $DXH(X)_nG\underline{D}XX\underline{D}(X)_nGN\underline{H}D/E$ (where n=~25 amino acids) whose active residues are a general acid catalyst (H124 in Glc7) and the carboxyl oxygen of two invariant aspartic acids (D91 and D94 in Glc7) (Goldberg et al., 1995). These residues are shown in Figure 2-1B (upper right panel). λ-PPASE is a bacteriophage ortholog of PP1 that is conserved in its catalytic domain with both human PP1 and Glc7 (Figure 2-1A) and has been previously used for structure-function analyses of the roles of the active residues in the PP1 catalytic pocket. Mutation of either D49 or D52 (D92 and D95 in PP1C-γ; D91 and D94 in Glc7) to a non-reactive asparagine residue (D>N), resulted in a catalytically dead enzyme in *in vitro* PPase assays. However, mutation of E59 (E>Q; E102 in PP1C and E101 in Glc7) reduced the catalytic activity of λ-PPASE ~8 fold and impaired Mn^{2+} recruitment, but did not significantly alter its substrate binding (Zhuo et al., 1994). An E>Q substitution in the equivalent residue of Glc7 (E101Q) is therefore predicted to reduce catalytic activity by perturbing the recruitment of the metal co-factor that enhances phospho-transfer, but not significantly change the shape or size of the Glc7 catalytic pocket (Figure 2-1B, lower right panel). Reduction of Glc7 catalytic activity in vivo, as a result of the E101Q mutation, would be expected to produce a recessive, hypomorphic *glc7* allele suitable for both 2D-DiGE and SGA analysis.

Figure 2-1: Structure of PP1 catalytic motif and the *glc7-E101Q* mutant

(A) PP1 protein phosphatases have highly conserved catalytic domains, consisting of residues acting as an acidic catalyst for phosphotransfer (CD1 and CD2) from the substrate and a phospho acceptor histidine residue (CD3). Residues in the catalytic pocket are highly conserved between human (PP1), yeast PPP-type PPases (Glc7 and others) and the bacterial PPase, λ-PPASE. **(B)** *Left panel*: The Glc7 catalytic pocket (pink) was modeled using the tertiary structure of human PP1C-γ (PDB Model 1jk7A; blue). *Right panels*: The E101Q mutation is predicted to inhibit the binding of a metal cation required to accelerate phospho-transfer to H124, but to not alter the shape/size of the catalytic pocket relative to wild-type Glc7.

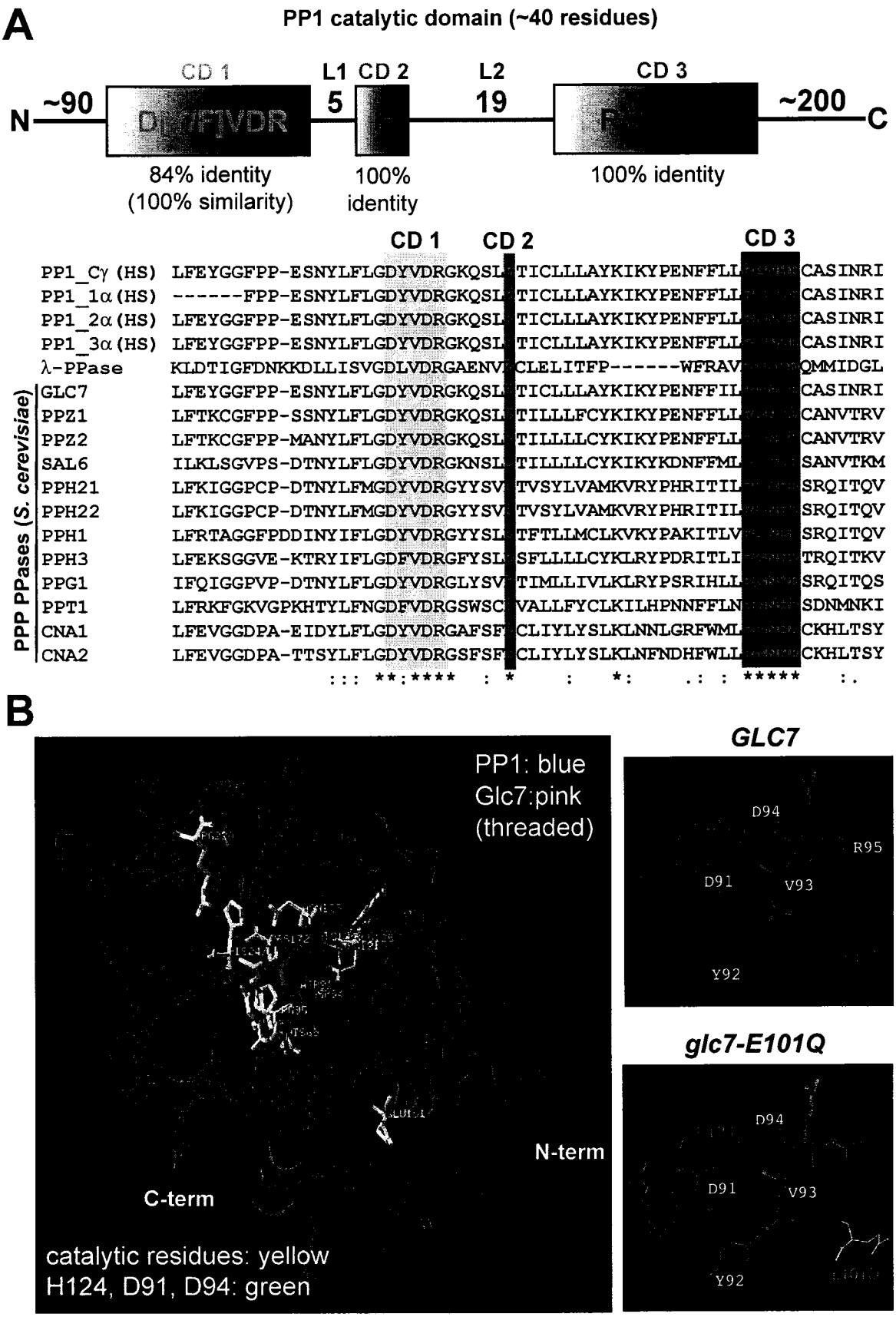
A
PP1 catalytic domain (~40 residues)
CD 1
L1
CD 2
L2
CD 3
N
~90
5
19
~200
C
84% identity
(100% similarity)
100%
identity
100% identity
CD 1
CD 2
CD 3
PP1_Cγ (HS) LFEYGGFPP-ESNYLFLGDYVDRGKQSL TICLLLAYKIKYPENFFLL CASINRI
PP1_1α(HS) ------FPP-ESNYLFLGDYVDRGKQSL TICLLLAYKIKYPENFFLL CASINRI
PP1_2α(HS) LFEYGGFPP-ESNYLFLGDYVDRGKQSL TICLLLAYKIKYPENFFLL CASINRI
PP1_3α(HS) LFEYGGFPP-ESNYLFLGDYVDRGKQSL TICLLLAYKIKYPENFFLL CASINRI
λ-PPase KLDTIGFDNKKDLLISVGDLVDRGAENV CLELITFP------WFRAV QMMIDGL
PPP PPases (S. cerevisiae)
GLC7 LFEYGGFPP-ESNYLFLGDYVDRGKQSL TICLLLAYKIKYPENFFIL CASINRI
PPZ1 LFTKCGFPP-SSNYLFLGDYVDRGKQSL TILLLFCYKIKYPENFFLL CANVTRV
PPZ2 LFTKCGFPP-MANYLFLGDYVDRGKQSL TILLLLCYKIKYPENFFLL CANVTRV
SAL6 ILKLSGVPS-DTNYLFLGDYVDRGKNSL TILLLLCYKIKYKDNFFML SANVTKM
PPH21 LFKIGGPCP-DTNYLFMGDYVDRGYYSV TVSYLVAMKVRYPHRITIL SRQITQV
PPH22 LFKIGGPCP-DTNYLFMGDYVDRGYYSV TVSYLVAMKVRYPHRITIL SRQITQV
PPH1 LFRTAGGFPDDINYIFLGDYVDRGYYSL TFTLLMCLKVKYPAKITLV SRQITQV
PPH3 LFEKSGGVE-KTRYIFLGDFVDRGFYSL SFLLLLCYKLRYPDRITLI TRQITKV
PPG1 IFQIGGPVP-DTNYLFLGDYVDRGLYSV TIMLLIVLKLRYPSRIHLL SRQITQS
PPT1 LFRKFGKVGPKHTYLFNGDFVDRGSWSC VALLFYCLKILHPNNFFLN SDNMNKI
CNA1 LFEVGGDPA-EIDYLFLGDYVDRGAFSF CLIYLYSLKLNNLGRFWML CKHLTSY
CNA2 LFEVGGDPA-TTSYLFLGDYVDRGSFSF CLIYLYSLKLNFNDHFWLL CKHLTSY
::: **:**** : * : *: .: : ***** :.
B
PP1: blue
Glc7:pink
(threaded)
N-term
C-term
catalytic residues: yellow
H124, D91, D94: green
GLC7
D94
R95
D91
V93
Y92
glc7-E101Q
D94
D91
V93
Y92

Introduction of a *glc7-D91N* mutation into haploid cells resulted in inviability (data not shown), consistent with this mutation resulting in a catalytically dead form of the enzyme *in vivo.* In contrast, *glc7-E101Q* strains were viable but uniformly exhibited slow growth in rich medium (YPAD) at 30˚C, with an average doubling time of 102 min in comparison to wild type reference strains (average of 81 min, R^2>0.95; Figure 2-2C). The growth of the *glc7-E101Q* strain was similar at 30˚C and 37˚C, indicating the *glc7-E101Q* mutant is not temperature-sensitive (data not shown). To determine if the slow growth phenotype of *glc7-E101Q* strains reflected a delay in cell cycle progression, mutant and wild-type cells in log phase cultures were harvested, stained with propidium iodide and DNA content measured by FACS analysis. This analysis revealed that proportion of G1, S, or M-phase cells in *glc7-E101Q* cultures was not statistically different from that of the wild type reference strains (Figure 2-2B). In addition, the proportion of unbudded, small-budded and large-budded cells was similar between wild-type and *glc7-E101Q* strains (Figure 2-2C). Finally, we wished to exclude the possibility that the E101Q mutation caused instability of the mutant Glc7 protein. Whole cell extracts were prepared from asynchronous cells expressing either Glc7-ProA or mutant *glc7-E101Q*-ProA fusion protein, and their relative abundance determined by 1D immunoblot analysis using anti-ProA antibodies. Actin was used as an internal standard for total protein loaded. The abundance of the *glc7-E101Q*-ProA mutant is not reduced relative to wild-type Glc7-ProA, suggesting that the slow growth of *glc7- E101Q* strains is not the result of protein instability (Figure 2-2D).

Figure 2-2: *glc7-E101Q* is a stable mutant which exhibits slow growth but no appreciable delay in the cell cycle

(A) The doubling time of wild type vs *glc7-E101Q* strains was determined from log-phase cultures. **(B)** FACs analysis for DNA content (propidium iodide staining) of log-phase wild-type and *glc7-E101Q* cells. Cell counts are shown plotted against fluorescence intensity (PI). **(C)** Doubling time (averaged over 4 hours, in minutes) and budding index of wild-type and glc7-E101Q mutant strains. **(D)** Western blot for Glc7-E101Q-ProA fusions compared to wild type (Glc7-ProA). Proteins from whole cell extracts (WCE) were separated by SDS-PAGE and blotted with anti-ProA mAb. Protein load is shown by immunoreactivity using anti-actin antibodies.

A

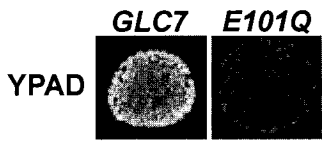

B

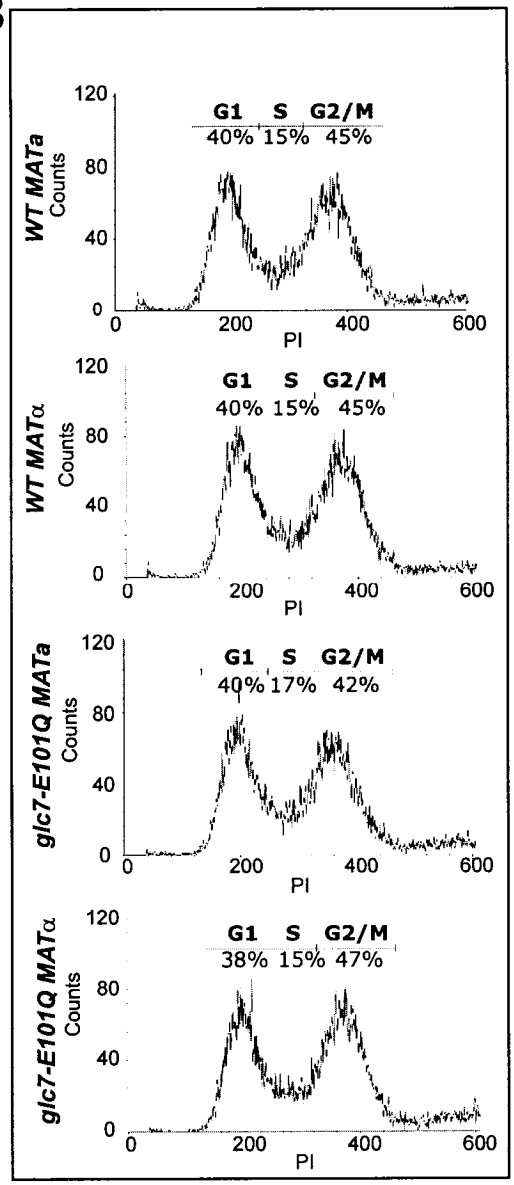

C

	strain			
	wild-type		*glc7-E101Q*	
	MATa	*MATα*	*MATa*	*MATα*
ave doubling (min) R^2>0.95	82	81	102	102

	budding index (%)		
strain	○	○○	○○
wild-type			
MATa (n=386)	52.3	26.2	21.5
MATα (n=408)	57.8	20.1	22.1
glc7-E101Q			
MATa (n=388)	58.8	19.1	22.1
MATα (n=365)	61.6	22.0	16.4

D

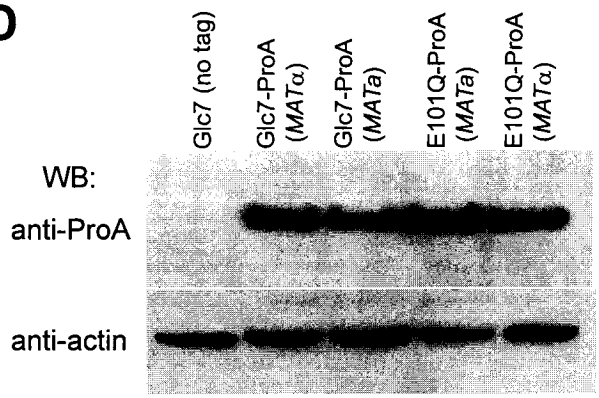

***glc7-E101Q* is impaired in glucose metabolism**

Glc7 has a well-established role in glucose metabolism. The first conditional allele of *glc7 (glc7-1)* (Stuart et al., 1994) was isolated as a consequence of its defect in accumulating glycogen in the presence of glucose, and other *glc7* mutants exhibit defects in glycogen accumulation and glucose sensing (Baker et al., 1997; Tu and Carlson, 1995). Glc7 was shown to play a direct role in the transcriptional repression of genes required for the metabolism of alternative carbon sources such as glycerol or ethanol. In the presence of glucose, Glc7 de-phosphorylates, and thereby inhibits, the Snf1 kinase responsible for transcription of these genes (Sanz et al., 2000b; Tu and Carlson, 1995). Additionally, Glc7 promotes glycogen accumulation in the presence of glucose by de-phosphorylating, and thereby activating, the glycogen synthase Gsy2 (Wu et al., 2001). Thus, growth on a non-fermentable carbon source such as glycerol, and the accumulation of glycogen in the presence of glucose are reliable reporters of Glc7 catalytic activity *in vivo*.

We hypothesized that the E101Q point mutation results in a hypomorphic *glc7* allele. If this were the case, *glc7-E101Q* would be expected to be deficient for growth on limited glucose (3% glycerol, 0.08% glucose; YPAG) and deficient in the accumulation of glycogen on rich medium (2% glucose; YPAD). We observed that the *glc7-E101Q* strain had a clear growth defect on YPAG relative to its growth on YPAD, and relative to the growth of the wild-type reference strain on YPAG (Figure 2-3A)

The poor growth of *glc7-E101Q* observed on limited glucose could be a petite phenotype resulting from mitochondrial mis-function. To test this possibility, tetrad analysis was performed on diploid cells heterozygous for *glc7-E101Q* in a genetic background homozygous for a defective *ade2Δ-101* gene. In the absence of adenine, *ade2Δ-101* cells accumulate P-ribosylaminoimidazole, an intermediate of the adenine

synthesis pathway. Mitochondrial oxidation of this intermediate results in a red pigment that colors colonies (Kim et al., 2002). We observed *glc7-E101Q* spore colonies consistently accumulated this red pigment on medium lacking adenine (Figure 2-3B), demonstrating the presence of functional mitochondria.

If *glc7-E101Q* is a recessive mutation and is the sole cause of the observed growth defects, a single copy of wild-type *GLC7* would be expected to rescue *glc7-E101Q* phenotypes. An un-linked copy of *GLC7* was integrated into the *URA3* locus (*GLC7-res*) of a *glc7-E101Q/GLC7* heterozygous strain, and haploid progeny obtained. Wild-type (*GLC7*), mutant (*glc7-E101Q*) and rescued (*glc7-E101Q GLC7-res*) progeny were scored for growth on YPAD versus YPAG. *glc7-E101Q* mutants containing *GLC7-res* were identified by their resistance to G418 and the ability to grow on medium lacking uracil (Figure 2-3C). As expected, *glc7-E101Q* cells exhibited a significant growth defect on both YPAD and YPAG relative to wild-type cells (Figure 2-3C). Additionally, the growth of *glc7-E101Q* cells on YPAG was reduced relative to their growth in the presence of glucose. However, the presence of *GLC7-res* restored growth of *glc7-E101Q* mutants on YPAD and YPAG to levels comparable to the wild-type reference strains.

Glycogen content in *glc7-E101Q* and wild-type strains was determined using iodine straining (Enjalbert et al., 2000). As with characterized *glc7* mutants (Baker et al., 1997; Stuart et al., 1994), *glc7-E101Q* cells grown on YPAD were deficient in glycogen content relative to the wild-type reference strains. This defect in glycogen accumulation was rescued by the presence of *GLC7-res* (Figure 2-3D). Taken together, these results strongly suggest that the *glc7-E101Q* mutation is a recessive allele and is hypomorphic for its catalytic activity *in vivo*.

Figure 2-3: ***glc7-E101Q*** **exhibits a slow growth defect and fails to accumulate glycogen in the presence of glucose**

(A) Growth of wild-type and *glc7-E101Q* strains was examined by spotting assays (~3000 cells/spot) grown in YPAD or YPAG for 48 hr at 30°C. **(B)** Spores derived from *glc7-E101Q/GLC7* diploids homozygous for the defective *ade2Δ-101* gene (YNS53) were examined for the presence of mitochondria. Red colonies are formed if functional mitochondria are present (wild-type condition) whereas white colonies are formed if mitochondria are lost (petite phenotype). **(C)** Tetrad analysis of meiotic progeny derived from the heterozygous diploid strain (*glc7-E101Q GLC7-res;* YNS128). Segregation of *glc7-E101Q* and *GLC7-res* were determined on selective medium (G418 and –uracil, respectively) and tetrad growth assessed on YPAD and YPAG medium. **(D)** Glycogen content was assessed in wild-type (*GLC7*), mutant (*glc7-E101Q*) and rescue (*GLC7-res*) strains by iodine staining. Brown color correlates with glycogen content.

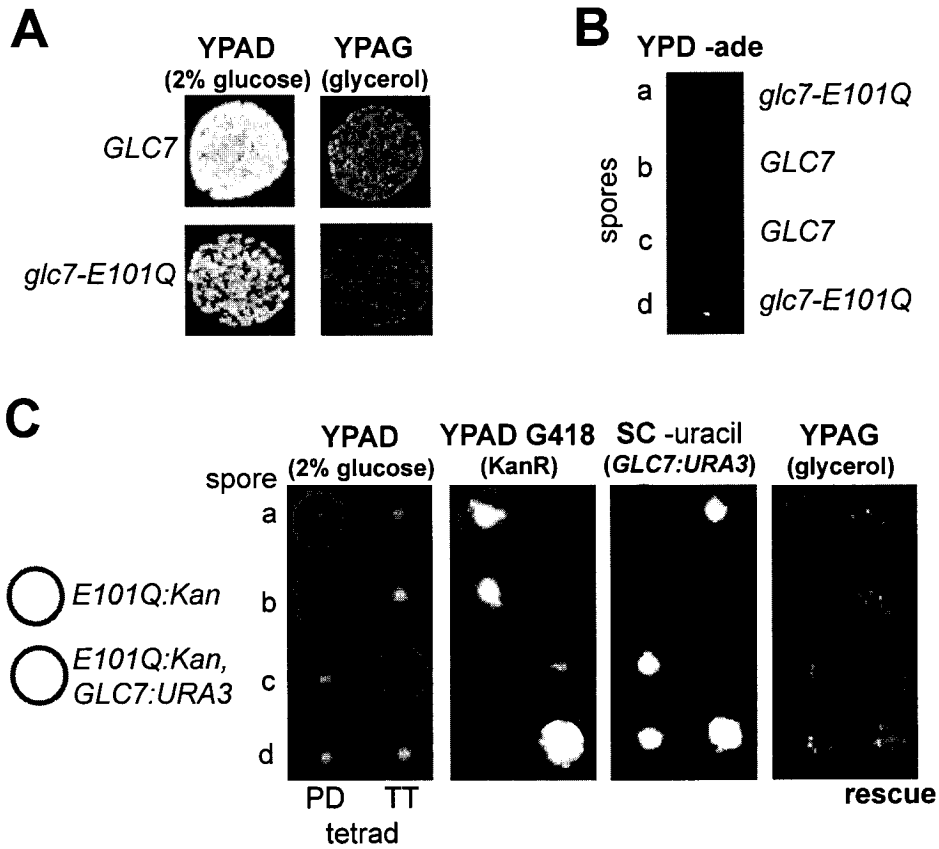
A
YPAD
(2% glucose)
YPAG
(glycerol)
GLC7
glc7-E101Q
B
YPD -ade
spores
a
b
c
d
glc7-E101Q
GLC7
GLC7
glc7-E101Q
C
YPAD
(2% glucose)
YPAD G418
(KanR)
SC -uracil
(GLC7:URA3)
YPAG
(glycerol)
spore
a
b
c
d
E101Q:Kan
E101Q:Kan,
GLC7:URA3
PD
TT
tetrad
rescue
D
Glycogen Content
(Iodine staining)
GLC7
glc7-E101Q
E101Q, GLC7:URA3
(MATa)
(MATα)
(MATa)
(MATα)
(MATa)
(MATα)
YPAD
(glu)

SGA analysis of *glc7-E101Q* reveals a broad genetic network encompassing Glc7-regulated processes

In order to expand the genetic network of Glc7 and to identify new candidate genes involved in Glc7-dependent processes, we screened ~4,700 non-essential genes for synthetic interactions with *glc7-E101Q* using the SGA methodology. Two types of genome-wide screens were performed to identify: (i) genes whose deletion impaired the growth of *glc7-E101Q* (synthetic sick/lethal: SSL) and (ii) genes whose deletion alleviated the growth defect of *glc7-E101Q* (synthetic rescue: SR). Two independent SGA screens were performed to 1) decrease the number of false negatives in the complete dataset and 2) to allow the second screen to act as a confirmation for the first (see Methods and Material for details). The two screens (each performed in triplicate) exhibited 60% and 39% identity, respectively, for SSL and SR genes identified. The total conserved network between the two SGA screens revealed 147 SSL and 178 SR interactions (Appendix, Table S3). Interacting genes were grouped into functional classes according to the GO (Gene Ontology) annotations deposited in the Saccharomyces Genome Database (SGD), and plotted in comparison to the frequency distribution of GO annotations in the deletion array (Figure 2-4). The biological processes enriched in the SSL screen included: protein biosynthesis, RNA and DNA metabolism, response to stress, transcription, cell cycle and meiosis. The SR screen was enriched for genes involved in transcription, organelle organization and biogenesis, protein modification, amino acid and derivative metabolism, cell budding, cytokinesis, and membrane organization. Both SSL and SR genes identified in the SGA encompassed numerous biological processes previously demonstrated to be Glc7-dependent: response to stress, transcription, cell cycle, meiosis, protein modification and cell budding (SGD database). These observations indicate that the *glc7-E101Q* mutant is defective in multiple aspects of Glc7 function.

Figure 2-4: Genetic network of synthetic sick/lethal (SSL) and synthetic rescue (SR) interactions with glc7-E101Q

The frequency distribution of synthetic sick/lethal (SSL) and synthetic rescue (SR) genes identified by SGA analysis of *glc7-E101Q*. Genes are assigned according to GO annotations (SGD database). The distribution of total genes screened in the SGA deletion array (Array) are shown for comparison.

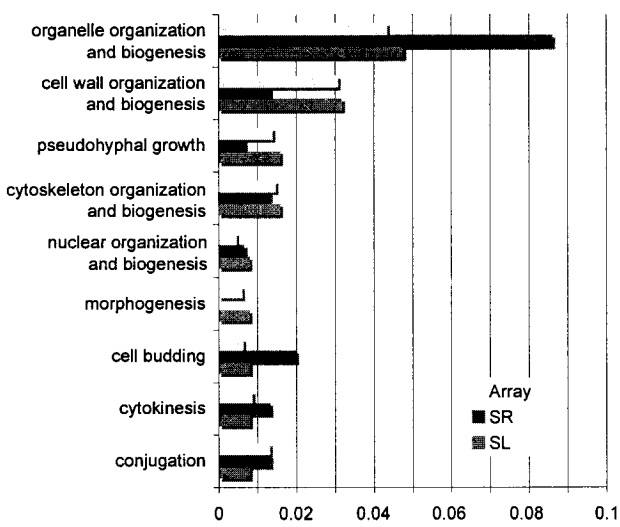
organelle organization and biogenesis
cell wall organization and biogenesis
pseudohyphal growth
cytoskeleton organization and biogenesis
nuclear organization and biogenesis
morphogenesis
cell budding
cytokinesis
conjugation
Array
SR
SL
0
0.02
0.04
0.06
0.08
0.1

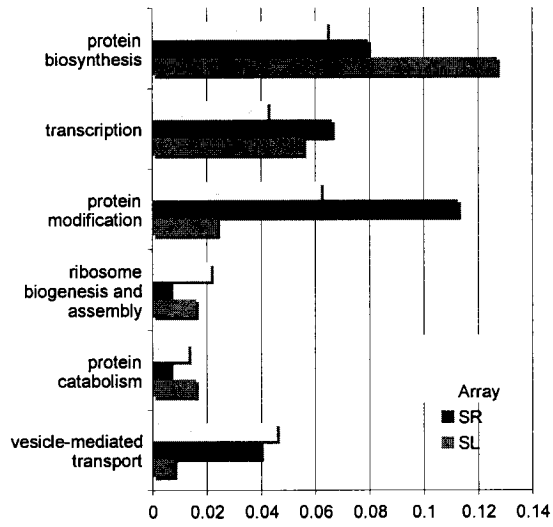
protein biosynthesis
transcription
protein modification
ribosome biogenesis and assembly
protein catabolism
vesicle-mediated transport
Array
SR
SL
0
0.02
0.04
0.06
0.08
0.1
0.12
0.14

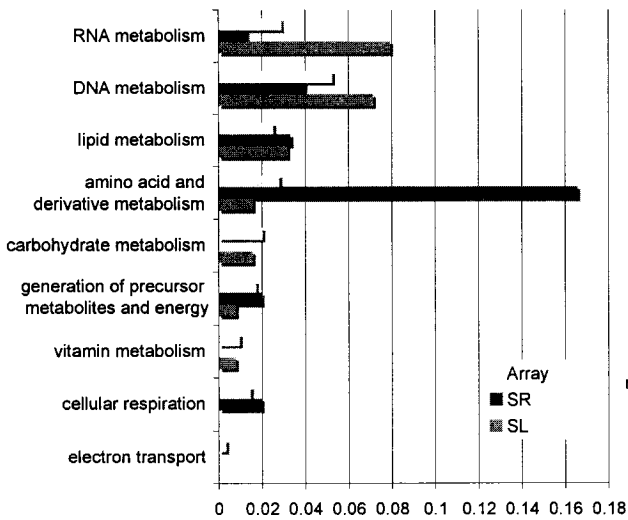
RNA metabolism
DNA metabolism
lipid metabolism
amino acid and derivative metabolism
carbohydrate metabolism
generation of precursor metabolites and energy
vitamin metabolism
cellular respiration
electron transport
Array
SR
SL
0
0.02
0.04
0.06
0.08
0.1
0.12
0.14
0.16
0.18

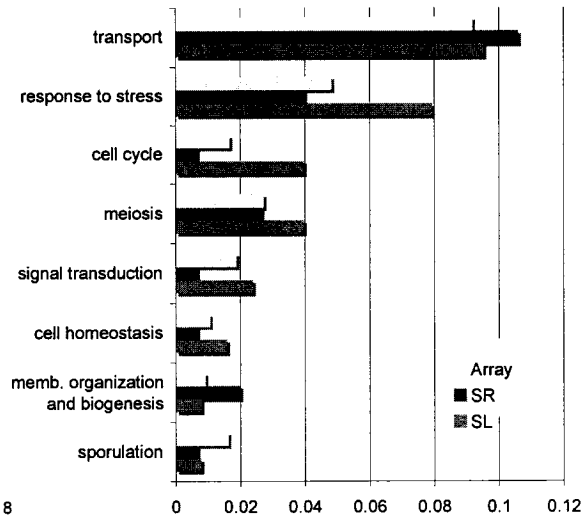
transport
response to stress
cell cycle
meiosis
signal transduction
cell homeostasis
memb. organization and biogenesis
sporulation
Array
SR
SL
0
0.02
0.04
0.06
0.08
0.1
0.12

The synthetic lethal interactions of *glc7-E101Q* were used in a cluster search using Funspec (Robinson et al., 2002), resulting in the identification of 4 clusters with a p-value<0.01 (Figure 2-5A). Clusters of genes acting in sister chromatid cohesion, chromatin silencing and co-enzyme metabolism were composed of relatively few genes, in contrast the cluster of genes acting in cell cycle (containing genes important for polarity, signal transduction, mating, karyogamy and budding) was large, suggesting Glc7 acts as a hub in this network.

To expand the *glc7-E101Q* synthetic lethal network, we searched for synthetic genetic interactions occurring in genes that show a genetic interaction with *glc7-E101Q*. A database search (BioGRID) revealed 32 SSL interactions among 21 such genes showing SSL interactions with *glc7-E101Q*. The resulting network shows the interplay between processes such as sister chromatid cohesion, Kar3, Kar9- or dynein-dependent nuclear migration, S-phase checkpoints and Cla4-mediated cell polarity (Figure 2-5B). All of these processes share SSL relationships with *glc7-E101Q*, indicating a key role for Glc7 in their regulation *in vivo*.

Figure 2-5: Glc7-dependent genetic interaction networks

(A) The 147 SSL interactions of *glc7-E101Q* were used in a cluster search as previously described (Robinson et al., 2002), resulting in the identification of 4 clusters with a p-value <0.01. Clusters are shown as bubbles whose diameter is proportional to the number of genes included in the cluster. **(B)** Synthetic lethal interactions among genes that are synthetic sick/lethal (SSL) with *glc7-E101Q*. The network of interactions was created using Osprey (v1.2) (Breitkreutz et al., 2003). Four key biological processes (nuclear migration, S-phase checkpoint, sister chromatid cohesion, and cell polarity) were shown to be functionally linked to Glc7 via their SSL interaction with *glc7-E101Q*.

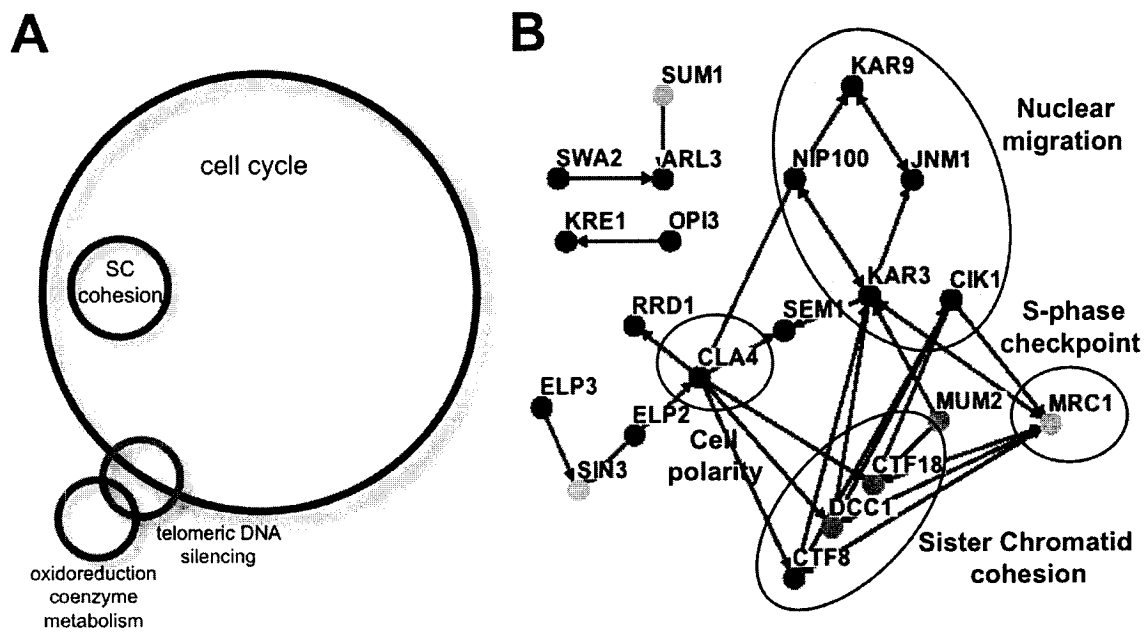
A
cell cycle
SC cohesion
telomeric DNA silencing
oxidoreduction coenzyme metabolism
B
SUM1
SWA2
ARL3
KRE1
OPI3
KAR9
NIP100
JNM1
Nuclear migration
KAR3
CIK1
RRD1
SEM1
S-phase checkpoint
CLA4
ELP3
ELP2
SIN3
Cell polarity
MUM2
MRC1
CTF18
DCC1
CTF8
Sister Chromatid cohesion

The enolase, Eno1, is mis-regulated in *glc7-E101Q* and is a suppressor of *glc7-E101Q* spore viability

The broad range of genetic interactions that we detected in the *glc7-E101Q* SGA, together with the large number of known protein-protein interactions (BIND) indicate that Glc7 is likely have many substrates *in vivo*. However, it is likely that the majority of these substrates remain unidentified. For this reason, we wanted to investigate changes in overall proteome complexity in the *glc7-E101Q* mutant relative to wild-type. Since Glc7 has a major role in glucose metabolism, we performed these analyses under growth conditions using YPAD (high glucose) or YPAG (glycerol). 2D-DiGE, which provides a sensitive method for detecting changes in protein abundance, isoforms and post-translational modifications, was employed for this analysis. We reasoned that the parallel analysis of data derived from three different sources; SGA, BIND and 2D-DiGE, could be used to identify candidate substrates and link them to specific functions or biological processes.

Multiplex 2D-DiGE was performed using proteins precipitated from whole cell extracts prepared from *glc7-E101Q* or wild-type strains grown at 30°C in the presence (YPAD) or absence of glucose (YPAG). Proteins (50 µg/sample) were labeled with Cy dyes (Cy3, Cy5 with Cy2 used for the pooled internal standard) using a reciprocal labeling method for triplicate samples (Unlu et al., 1997). 2D-PAGE was performed as described in Materials and Methods. The spot file generated in Decyder 6.5 contained 980 proteins (Figure 2-6A). Proteins whose abundance significantly changed in the context of the four conditions (carbon source: YPAD or YPAG) or strain (*glc7-E101Q* versus wild-type) were identified using 2 way-ANOVA (DeCyder BVA module; p-value ≤0.01). This analysis revealed 39 proteins changed as a consequence of both the strain and the carbon source (interaction; Glc7 and carbon source dependent), 70 proteins

changed as a consequence of the strain (carbon source-independent), and 149 proteins changed as a consequence of the carbon source (Glc7 independent).

2D-DiGE analysis revealed the non-essential enolase, Eno1 changed as a consequence of both the *glc7-E101Q* mutation and the carbon source (Figure 2-6A). Eno1 and the essential enolase Eno2 are phosphopyruvate hydratases that catalyze the conversion of 2-phosphoglycerate to phosphoenolpyruvate during glycolysis and the reverse reaction during gluconeogenesis. This second reaction is important for growth on alternative carbon sources such as ethanol and glycerol (Entian et al., 1987; McAlister and Holland, 1982). Transcription of *ENO1* and *ENO2* is generally repressed in the presence of glucose, however log phase cells contain approximately 20-fold more Eno2 than Eno1 (McAlister and Holland, 1982). *ENO1* is up-regulated in alternative carbon sources, leading to Eno1 levels equivalent to Eno2 (Ferea et al., 1999; Roberts and Hudson, 2006). Several isoforms of Eno1 (eno1_A [spot#533], eno1_B, eno1_C) were identified by LC-MS/MS (QTRAP) (Figure 2-6B and supplementary Table S4). Of the three Eno1 isoforms, only eno1_A exhibited Glc7 and carbon-dependent changes in abundance ($p=0.003$; Figure 2-6A). The relative abundance of eno1_A in wild-type cells grown in glucose versus glycerol was consistent with glucose repression; Eno1 abundance was low in cells grown in YPAD but increased in cells grown in YPAG (Figure 2-6C). In contrast, eno1_A abundance was increased in *glc7-E101Q* cells grown in glucose relative to wild-type (Figure 2-6C). Spots in the Eno1 cluster were changed as a consequence of both strain and carbon source, and were consistent with glucose repression and up-regulation in YPAG (data not shown). Taken together, results suggested Eno1 stability or expression might be altered in the *glc7-E101Q* mutant.

A null mutation of *ENO1* (*eno1Δ)* was identified as a SR interaction in the *glc7-E101Q* SGA (Appendix, Table S3). We therefore asked if the *eno1Δ* mutation might alleviate the defect in glycogen accumulation observed in *glc-E101Q* cells grown in the

presence of glucose. However, this was not the case (Figure 2-6D), suggesting the *eno1*Δ SR interaction was not directly linked to Glc7's function in glycogen synthesis or glucose metabolism.

The genetic interaction network obtained with the *glc7-E101Q* SGA revealed that Glc7 is functionally linked to several aspects of the sexual cycle; in the formation of mating projections, in karyogamy and in meiosis (Figures 2-4 and 2-5). Heterozygous diploids, resulting from mating a *glc7-E101Q* haploid strain with a wild-type strain, produced fewer (30%) haploid progeny than diploids resulting from mating a *glc7-E101Q* haploid strain containing a copy of *GLC7 (GLC7-res)* with a wild-type haploid strain (94%; Figure 2-6E), thus involving Glc7 in spore viability. We asked if an *eno1*Δ mutation would alleviate this spore viability defect, and found that when *glc7-E101Q* *eno1*Δ haploids were mated to wild-type, the resulting diploids produced 77% viable progeny (Figure 2-6E). These results suggested that increased spore viability, rather than a rescue of defects in glycogen accumulation, was a basis for the SR phenotype of the *glc7-E101Q* *eno1*Δ double mutant.

Figure 2-6: Enolase-1 (Eno1) is mis-regulated in *glc7-E101Q* and rescues low spore viability but not glycogen accumulation defects in *glc7-E101Q*

(A) Identification of protein modifications by medium resolution 2D-DiGE gel analysis. Changes in protein abundance relative to a) *glc7-E101Q* relative to wild type and, b) growth in different carbon sources (YPAD and YPAG) was determined. A list of 980 spots was generated and changed proteins identified according to strain, carbon source or the interaction of both using 2-way ANOVA ($p \leq 0.01$; Decyder Software BVA module v6.5.) The number of changed spots in each category (interaction, strain, carbon source) is shown, and the significance (p-value) for three isoforms of the enolase, Eno1 (eno1_A-C) are shown. **(B)** Representative gels showing Eno1 isoforms and their context to the spot map (eno1_A-C). *Upper panel*: gel containing Cy3-labeled sample derived from wild-type cells grown in YPAD. *Lower panel:* Merged image of a deep-purple stained gel (total protein) overlaid with that of the synthetic image of the pooled standard (Cy2-channel). Spot #533 (eno1_A) was significantly altered in the interaction and carbon source categories. **(C)** Log-standardized fold intensity changes for eno1_A (spot 533) in wild type and *glc7-E101Q* grown in YPAD or YPAG (n=3 biological replicates/strain, condition). **(D)** Glycogen content was assessed in wild-type (*GLC7*), *glc7-E101Q* and *glc7-E101Q eno1Δ* strains by iodine staining. Brown color correlates with glycogen content. **(E)** The *eno1Δ* mutation suppresses a defect in spore viability observed for the *glc7-E101Q* mutant.

A

spots (total)	spots in category (p<0.01)		
	interaction	strain	carbon source
980	39	70	149

	p-value		
	interaction	strain	carbon source
eno1_A	0.003	0.066	<0.001
eno1_B	0.110	0.058	0.022
eno1_C	0.041	0.004	0.012

B

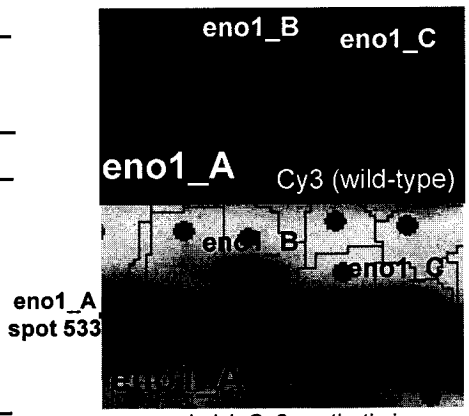

C

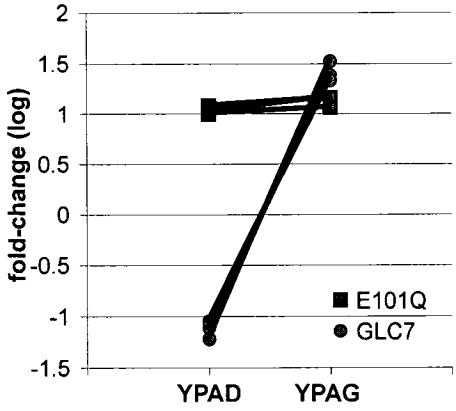

D

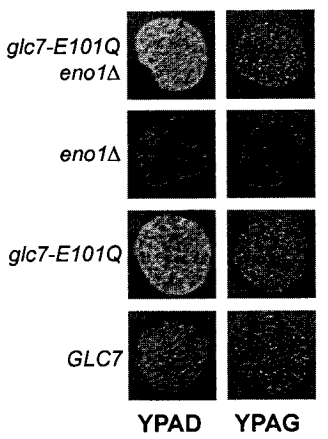

E

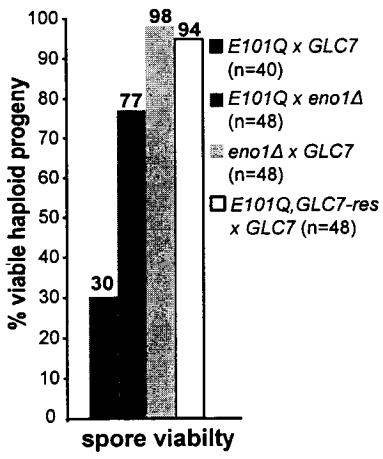

2.4. Discussion

Glc7 and the dual-specificity PPase Cdc14 are the only essential PPases of budding yeast, and are both likely to act as major signaling hubs. To date, neither PPase has been examined using large-scale genetic or proteomic approaches. In the case of Glc7, the number of known genetic interactions (~20) are greatly exceeded by the number of protein-protein interactions (~100) detected in two-hybrid and affinity capture screens (SGD) (Gavin et al., 2002; Ho et al., 2002). As a result of this disconnect between genetic and proteomic data, little information is available for the Glc7 signaling network. However, the large number of protein-protein interactions and phenotypes in numerous cellular processes suggests Glc7 has a large and complex signaling network. In combination with previous characterization of Glc7's localization and mutant phenotypes, large-scale analysis of genetic interactions and proteome complexity has the potential to reveal novel aspects of Glc7 function and provide greater understanding of its signaling interactions *in vivo*.

Existing conditional *glc7* alleles contain mutations which lie outside of the Glc7 catalytic domain and alter the binding of regulatory subunits that provide substrate specificity (Andrews and Stark, 2000; Baker et al., 1997; Knaus et al., 2005; Ramaswamy et al., 1998; Tu and Carlson, 1995). As a result, these mutations may perturb very specific aspects of Glc7 function and thus only reveal a subset of Glc7's genetic and proteomic interactions. We postulated that a single point mutation within the catalytic domain of Glc7, predicted to impair phosphate transfer but not substrate or adaptor binding, would result in a hypomorphic allele that is well suited for large-scale analyses. The *glc7-E101Q* mutant appears to be a generalized hypomorph; this mutant exhibits defects in glucose metabolism consistent with decreased catalytic activity but also exhibits a broad range of genetic interactions that include known functions of Glc7. Finally, we hypothesized that a combined approach in genetics (SGA) and proteomics

(2D-DiGE) would allow for the identification of new Glc7 substrates and/or Glc7-regulated proteins that either single analysis may not detect.

Analysis of synthetic genetic interactions using the SGA, combined with a high-resolution map of changes in the proteome using 2D-DiGE, has the potential to provide biologically significant links between genes and proteins. For example, SGA analysis reveals a Glc7-dependent network in polarity based on a Cla4 hub (Figure 2-5B). Pkc1 functions in the polarity network (GO), but has no direct physical link to Glc7 (Figure 2-7). 2D-DiGE analysis revealed mis-regulation of Eno1, which physically interacts with both Glc7 and Pkc1, and genetically with the *glc7-E101Q* mutant (Figure 2-7). In the absence of both analyses, the relationship between Glc7, Pkc1 and Eno1 and its biological significance may well have remained undetected.

Eno1 was identified as a SR of *glc7-E101Q*, and a mis-regulated protein in *glc7-E101Q* cells grown in glucose. These two observations led us to investigate the SR interaction between *glc7-E101* and *eno1*Δ in detail. We found that the SR interaction was the consequence of increased spore viability. There are several possible explanations for this result. First, Eno1 physically interacts with Glc7 (Graumann et al., 2004) and thus may be a substrate. Second, inappropriate regulation of Eno1 in the *glc7-E101Q* mutant, either at the transcription and/or post-translational level, may perturb glucose metabolism. In this scenario, deletion of mis-regulated Eno1 would alleviate the defect. A formal possibility is that Eno1 may have a Glc7-dependent function in glucose metabolism that is particularly important during sporulation. Spore viability can be viewed as a complex readout of the combination of multiple signaling pathways linked to Glc7 and Eno1; Pkc1 (GO: cell wall synthesis), Smt3 and Ard1 (GO: meiosis) (Figure 2-7). A recent study has implicated Eno1 and Eno2 in membrane fusion, suggesting these enzymes may have additional, non-metabolic functions (Decker and Wickner, 2006). Thus, an intriguing possibility is that the interaction between Glc7

and Eno1 is important for integration of glucose metabolism with other signaling networks involved in spore formation.

Figure 2-7: Protein interaction network of Eno1 indicates a potential non-metabolic role in spore viability

Physical interactions shared between Eno1 and Glc7 were mapped according to SGD (BioGRID) and are shown according to GO annotation. Pkc1, Ard1 and Smt3 share physical interactions with Eno1 and each has been shown to play regulatory roles in meiosis and/or spore viability. This observation, combined with the physical interaction of Glc7 with Eno1, suggests a Glc7-dependent role for Eno1 in spore formation.

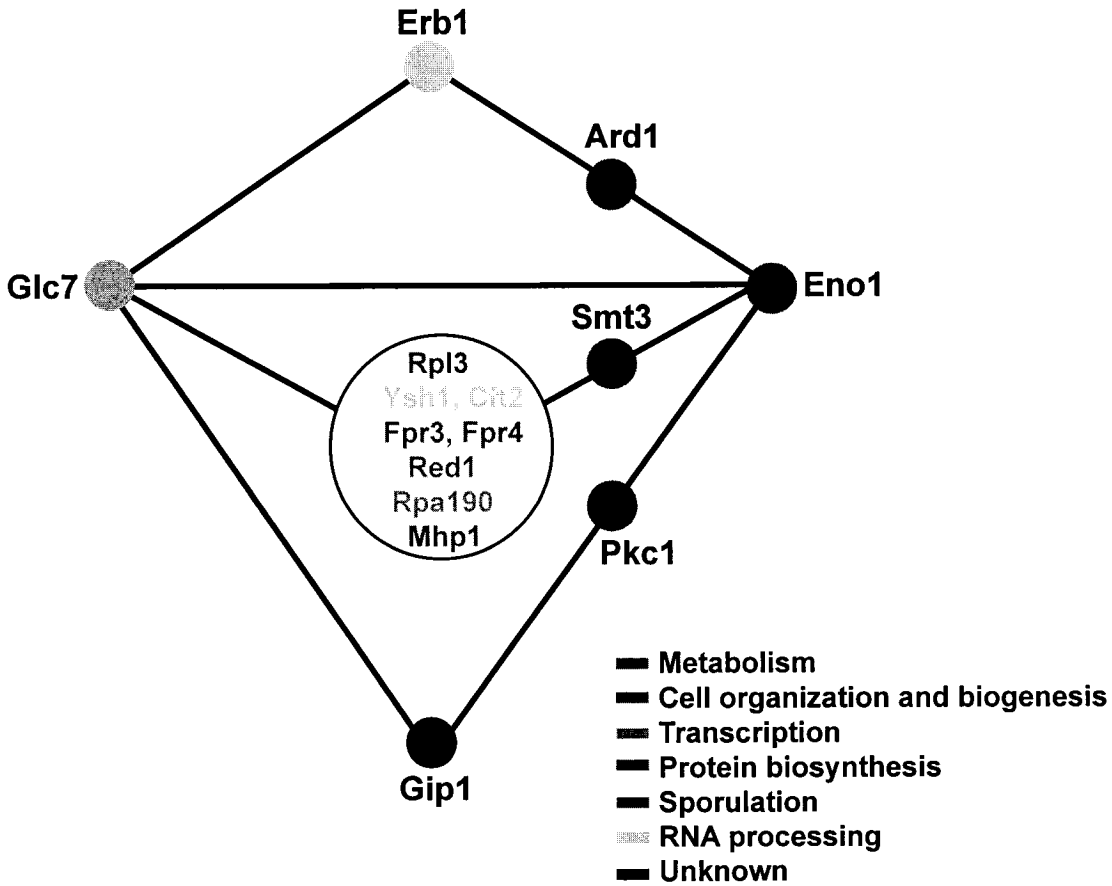
Erb1
Ard1
Glc7
Eno1
Smt3
Rpl3
Ysh1, Crt2
Fpr3, Fpr4
Red1
Rpa190
Mhp1
Pkc1
Gip1
Metabolism
Cell organization and biogenesis
Transcription
Protein biosynthesis
Sporulation
RNA processing
Unknown

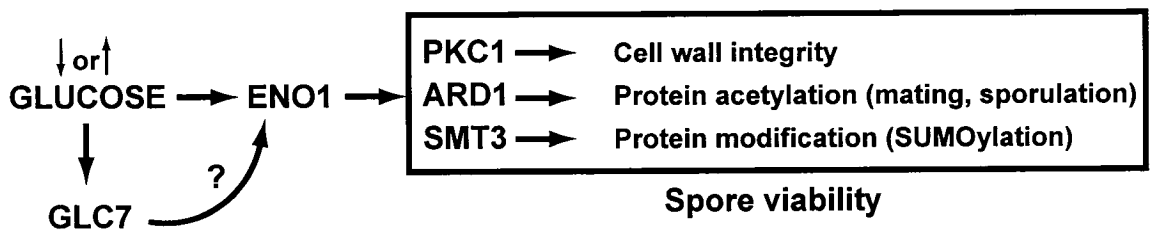
or
GLUCOSE
ENO1
GLC7
?
PKC1
Cell wall integrity
ARD1
Protein acetylation (mating, sporulation)
SMT3
Protein modification (SUMOylation)
Spore viability

2.5. Acknowledgements

We thank Damien D'amours, Phil Branton, Malcolm Whiteway and all the members of the Vogel, Mandato and Bussey labs for fruitful discussions and support during this project, and acknowledge the Cell Imaging and Analysis Network (CIAN) DiGE and SGA platforms. JV is supported by a New Investigator Award from the Canadian Institutes of Health Research (MSH 69117). This research was supported by operating grants from the Canadian Institutes of Health Research (MOP-64404 to JV and MOP-68970 to CM), the Natural Sciences and Engineering Research Council (262246-03 to JV and 6040-03 to HB) and infrastructure grants from the Canada Foundation for Innovation to awarded to JV (CFI 7395) and to the Developmental Biology Research Initiative of McGill University (CFI 8298).

Chapter 3: General discussion

In this study we have presented a novel approach to discover biologically relevant interactions between PPases and the pathways they regulate. To date, a limited amount of information about yeast PPases has emerged from large screens and small-scale biochemical studies do not provide satisfactory information to build a biologically significant network. We reasoned that PPase signaling networks could be identified through parallel large-scale analysis of genetic and physical interactions. We hypothesized that the use of structurally intact catalytic PPase mutants capable of properly interacting with their phospho-regulatory networks along with integration of complementary proteomic and genomic approaches would facilitate the creation and validation of a global network of genetic and physical interactions.

Based on previous *in vitro* studies and our structural analysis of Glc7 we created the *glc7-E101Q* allele. We hypothesized that changing single amino acids in the catalytic phosphoesterase domain while preserving the overall structure of the pocket should theoretically decrease Glc7 catalytic activity without compromising enzyme structure. *In vivo,* the epitope tagged version of the mutant allele was expressed at levels comparable to wild-type Glc7 suggesting that defects observed in the E101Q strains are caused by its catalytic deficiency. Thus the observed *glc7-E101Q* phenotypes are not the result of structural instability, which inevitably leads to defective physical interactions with its binding partners. Using previously established assays, the *glc7-E101Q* allele displayed a wide range of phenotypes, normally associated with multiple defects in binding to several known regulatory subunits involved in glucose metabolism, glycogen synthesis and chromosomal stability. These phenotypes are specific to *glc7-E101Q* as the integration of the *GLC7-res* construct in the mutant strains eliminated these defects. Interestingly, because of the hypomorphic nature of the allele, some known defects observed in structurally compromised *glc7* alleles were not observed. For example, the

FACS analysis and bud index of *glc7-E101Q* did not show a specific cell cycle delay despite the previously observed G2/M arrests in a number of conditional *glc7* alleles at non-permissive temperature (Bloecher and Tatchell, 1999; Hisamoto et al., 1994; MacKelvie et al., 1995). There are several possible explanations for the lack of G2/M delay observed in the *glc7-E101Q* mutant. First, the *E101Q* allele is partially active (catalytic hypomorph), and it is formally possible that the genetic buffering for some of its functions may be more efficient and thus this allele would have a constrained spectrum of scorable defects. Second, the partial catalytic activity of *glc7-E101Q* may be sufficient to maintain regulation of a subset of Glc7 cellular targets, for example those involved in mitosis and chromosome segregation. If true, this may suggest that there is a biological threshold that must be reached in order to disrupt certain pathways. The relative levels of Glc7 and Ipl1 are important for maintaining a balanced phospho-regulatory function, thereby insuring accurate chromosome segregation (Cheeseman et al., 2002). For instance, a subset of Ipl1 dosage suppressors are cytoplasmic Glc7 interacting proteins. When overexpressed, these interactors alter Glc7 localization and restore the nuclear Glc7/Ipl1 phospho-regulatory balance in the mutant background (Pinsky et al., 2006). In addition, conditional alleles of the essential Glc7 nuclear regulatory subunit *SDS22,* involved in chromosome stability and mitosis, which retain reduced ability to interact with Glc7 (Ceulemans and Bollen, 2004; Peggie et al., 2002) also rescue growth defects associated with *ipl1* alleles. Interestingly, these alleles do not trigger a checkpoint at non-permissive temperature, but rather are inviable because of the rate at which cells become aneuploid (Peggie et al., 2002). Since *glc7-E101Q* is structurally stable and maintains protein levels similar to wild-type cells, it is possible that the remaining catalytic activity enables the cell to retain partial regulatory function of specific pathways and maintain progression through the cell cycle. Third, Glc7 may act both as a regulator of effectors of spindle assembly and kinetochore function (chromosome segregation)

and as a regulator of the checkpoint mechanism itself; for example Glc7 may regulate Ipl1 (which is required for checkpoint function) (Cheeseman et al., 2002; Francisco and Chan, 1994; Pinsky et al., 2006) or checkpoint effectors such as Mad1-3 or Bub1 or Bub3 (Chen et al., 2004). These checkpoint proteins were not detected as SSL interactors in the *glc7-E101Q* SGA analyses, which is consistent with the mutation compromising checkpoint function. Fourth, and finally, the chromosome instability (CIN) of the *glc7-E101Q* mutant has not yet been formally tested using CIN assays such the sectoring of a artificial chromosome fragment. Sectoring assays are currently being performed to test directly and quantitatively for CIN in the *glc7-E101Q* mutant strain.

We queried the synthetic genetic array composed of the ~4700 non-essential yeast gene knockouts to identify genes interacting with *glc7-E101Q*. In comparison to the previously established dataset of 26 *glc7* genetic interactions (BioGRID), the usage of the *glc7-E101Q* allele has improved the mining capacity of the SGA with a yield of 147 SSL and 178 SR interactions. The broad spectrum of synthetic genetic interactions suggests that the *glc7-E101Q* allele is compromised in several aspects of *GLC7* function. The 147 SSL interactions were analyzed for the presence of functional clusters (GO annotation) using Funspec, a clustering tool that calculates the probability that the intersection of a gene list with any given functional category occurs by chance (Robinson et al., 2002). This analysis resulted in the identification of four statistically significant clusters of genes based on GO annotation. Genes in these functional clusters are implicated in the *GLC7* signaling network with an emphasis on genes acting in cell cycle (polarity, signal transduction, mating, karyogamy and budding).

To complement the genetic network derived from the SGA results, we employed 2D-DiGE, a proteomic analysis tool that permits the quantitative comparison of proteome-wide changes with statistical confidence (Unlu et al., 1997). 2D-DiGE analysis of changes in the *glc7-E101Q* mutant proteome under fermentation and obligatory

aerobic conditions revealed alterations in the stability and expression levels of numerous proteins. Multi-variable analysis of variance (2-way Anova) enabled us to flag spots with altered expression patterns due to *glc7-E101Q* (strain; condition 1), growth media (carbon source; condition 2) or the interaction between both conditions (synergistic effect; condition 1 + condition 2). The interaction p value is of particular interest as it indicates a relationship between strain and carbon source. Statistical significance in this category suggests *glc7-E101Q* dependent regulatory defects within the metabolic network. This dataset contained 39 spots and included spot 533, later identified as Eno1_A.

The integration of the generated genetic and proteomic data along with the complementary information from published interaction datasets (BioGRID) (Breitkreutz et al., 2002) facilitated the identification of a null mutation (*eno1Δ*) in the *ENO1* gene as a suppressor of *glc7-E101Q* and suggested a novel non-metabolic role for Eno1 in the Glc7 interaction network. The SGA analysis contained *eno1Δ* as a SR interaction with *glc7-E101Q* and our proteomic 2D-DiGE analysis revealed that Eno1 (Eno1_A, spot 533) was mis-regulated in *glc7-E101Q* cells grown on glucose. Subsequently, the genetic rescue interaction was confirmed by showing that *eno1Δ* increased spore viability by almost 2 fold in the meiotic progeny of the heterozygous diploid double mutant strain (*glc7-E101Q/GLC7*, *eno1Δ/ENO1*). This result suggests that the observed increase in spore viability is the basis for the SR phenotype of the *glc7-E101Q/eno1Δ* double mutant.

Spore viability is a basic readout for many cellular processes such as chromosome segregation, metabolism and cell wall synthesis, indicating that Eno1 may have multiple functions. Interestingly, Eno1 interacts physically with Glc7 as well as with Ard1, Pkc1 and Smt3 *in vivo* (Figure 2-7). This high-throughput interaction data partially

concurs with post-translational modification prediction tools, which indicate a significant probability of Eno1 being phospho-regulated (NetPhos/K) (Blom et al., 2004) and SUMOlated (SUMOplot) (Xue et al., 2006) but do not show evidence of N-terminal acetylation sites (NetAcet) (Kiemer et al., 2005). In addition, N-terminal acetyl transferase forms a homodimer composed of Ard1-Nat1 (Park and Szostak, 1992) and the latter is absent from Eno1 physical interaction data. However, the regulatory functions of Ard1 in mating and sporulation (both deficient in *glc7-E101Q*) along with its physical interactions suggest a biologically relevant function in the Eno1 interaction network. Since Nat1 was not identified, this may indicate a function independent of Ard1's primary enzymatic function. Testing whether Eno1 or Glc7 are N-terminally acetylated *in vivo* would be a first step in determining the biological significance of the *glc7-E101Q ard1*Δ interaction. The combination of previously published high-throughput data for Eno1 with our results opens the possibility for Eno1 acting in a non-metabolic fashion- perhaps as a sensor or a scaffold which provides a read out of metabolic state or links the metabolic components of the cell to pathways driving the cell cycle. It is also possible to speculate that Glc7 with Pkc1 and Smt3 regulate Eno1 through post-translational modifications. This putative function of Eno1 may be perturbed in *glc7-E101Q* cells either at the post-translational and/or transcriptional level, falsely signaling a metabolic deficiency within the cell, which in turn affects energy expenditure for cell growth and cell wall formation. When the sensor function provided by Eno1 is abrogated (*eno1Δ*), there may be no readout and the cell may divert as much energy as required into these functions, which is ultimately reflected in increased spore viability.

To further investigate the proposed non-metabolic regulatory mechanism involving Glc7 and Eno1 we need to clearly assess if Eno1 is modified post-translationally in a Glc7 dependent manner and subsequently whether these modifications are altered in *glc7-E101Q* cells. It is intriguing to speculate that altered

phosphorylation of Eno1 in *glc7-E101Q* cells increases protein stability. Epitope tags can be used to assess regulation (PTMs) of Eno1. The epitope tagged Eno1 can be used for 2D immunoblots taking advantage of narrow range IPG strips to enhance isoform resolution. This would be done with extracts from cells grown under the same set of conditions used in the DiGE study. Altered isoforms of Eno1 found to be *glc7-E101Q* dependent would further support the proposed non-metabolic regulatory role of Eno1 in the Glc7 interaction network. A phosphatase treatment to collapse these additional isoforms would be required to confirm that these changes in mobility in the first dimension are due to phosphorylation.

Combining these results with expression profiling data is key to gain more insight into how Eno1 becomes mis-regulated in *glc7-E101Q cells*. This method would enable us to analyze the global transcription profile of *glc7-E101Q* cells under the same growth conditions used for 2D-DiGE using a micro-array chip containing all yeast ORFs (~6000) (Enjalbert et al., 2003). With a larger set of identified protein spots from 2D-DiGE, this additional layer of data would allow a more thorough understanding of the Glc7 regulatory network by differentiating between alterations in the proteome caused by changes in gene expression from alterations caused by changes in post-translational modifications affecting protein stability. In this particular study, it may show if the mis-regulation of Eno1 in *glc7-E101Q* cells grown on glucose is due to changes in Eno1 transcription or if Eno1 stability is altered, possibly through a mechanism involving Glc7 and Smt3.

Our preliminary findings using the *glc7-E101Q* allele have provided a road map for further investigation and optimization of our methodology for uncovering PPase functions. A well-known caveat of the SGA analysis is the under-representation of genes involved in karyogamy and other mating related functions (Tong et al., 2001). Since *glc7-*

E101Q interacted genetically with genes involved in these processes, our SGA analysis may have generated an incomplete picture of the *glc-E101Q* genetic interaction spectrum. Therefore, the SGA methodology should be modified in order to use the *glc7-E101Q* query strain with the integrated *GLC7-res* construct (*ura3::GLC7:URA3*) to bypass any mating deficiencies. This modification requires an additional reagent to select against the extra copy of *GLC7* (*URA3+*) before the final viability readout of haploid double mutant spores. A simple solution is to include 5-Fluoroorotic Acid (5-FOA) that selects against *URA3+* cells (Boeke et al., 1984) prior to the final double mutant selection step.

It would be also interesting to see how the synthetic interactions are altered on different growth media by including in the SGA a comparison of fitness on glucose and glycerol media. This additional analysis would reveal where the metabolic machinery fails to switch efficiently to aerobic metabolism in *glc7-E101Q*.

The DiGE datasets generated in this study did not permit efficient detection of changes specific to the phospho-proteome nor provided means to rapidly distinguish them from the rest of the statistically significant changes. Counterstaining of DIGE gels with the Pro-Q Diamond reagent that labels specifically phosphoproteins has been shown to enable quantitative detection of phosphoproteins in 2D gels (Stasyk et al., 2005). Previous preliminary 2D electrophoresis of the phospho-proteome of *glc7-E101Q* and wild type cells stained with phospho-specific Pro-Q Diamond dye, revealed a general increase in abundance of phospho-proteins in the *glc7-E101Q* background (Michael Logan, unpublished data). The integration of Pro-Q Diamond counterstaining into the 2D-DiGE workflow would allow us to correlate protein spots with altered abundance based on DiGE analysis with changes in phosphorylation levels from the Pro-Q Diamond counterstained gels. This type of analysis would be of particular interest, as it may point towards candidate proteins involved more directly in the Glc7 phospho-

regulatory network. In addition, the dimensions of the 2D-DiGE gels used (13cm x 18cm) combined with the wide range strips may be of insufficient resolution to appreciate the changes in the phospho-proteome. Using a larger format for the 2D-DiGE electrophoresis (24cm x 28cm) along with use of strips with a narrower pH range may increase the resolution of this analysis within a particular pH window of interest and reveal more clearly the phospho-specific isoforms.

The dataset of 2D-DiGE protein spots analyzed by MS is insufficient in size to clearly indicate to what extent the integration of the generated genetic (SGA) and proteomic data (2D-DiGE) enhances our understanding of the Glc7 regulatory network. Previous analysis of the yeast genetic and protein-protein interaction networks from published datasets revealed that the number of common neighbors between two genes in a genetic network correlates with a known protein-protein interaction between the corresponding gene products and increases in statistical significance with the number of shared genetic interactions (Tong et al., 2004). This suggests that there should be a partial overlap between large datasets. In the case of Glc7, our genetic analysis resulted in a large dataset of 147 SSL and 178 SR interactions that led the identification of four statistically significant clusters of genes based on GO annotation. Moreover, published high throughput two-hybrid and affinity capture screens indicate over a hundred protein-protein interactions with Glc7 (BioGRID). Therefore, integrating the genetic and proteomic Glc7 datasets should generate a filtered dataset of matched genetic and protein-protein interactions that are linked to Glc7 function. This approach will establish a pipeline of biologically relevant interactions to be further analyzed and facilitate the confirmation process of the Glc7 signaling network identified through the parallel large-scale analysis of genetic and physical interactions.

Given the complete conservation of the catalytic pocket amongst the PPP family of serine/threonine PPases in *Saccharomyces cerevisiae*, the methodology presented in this thesis can be easily adapted to the other members of the PPP family by engineering catalytic mutants harboring a mutation equivalent to E101Q in *GLC7*. However, because of the non-essential nature of these PPases, each catalytic hypomorph should be used in a carefully engineered genetic background where the other highly related PPPs are deleted. This will ensure scorable phenotypes by reducing genetic buffering amongst highly related PPases.

In addition, this methodology may also be adapted to study Cdc14, the other essential PPase in budding yeast. This evolutionarily conserved DSP is the central effector of the mitotic exit network (MEN) and the Cdc fourteen early anaphase release (FEAR) network. Upon activation, Cdc14 regulates several key events that occur during anaphase, such as chromosome segregation, mitotic spindle stability and initiation of mitotic exit. The proper coordination of these events is key for genomic stability (D'Amours and Amon, 2004; Saunders, 2002). Similarly to the PPP family, the catalytic domain of PTPs/DSPs is well conserved and contains invariant residues forming the catalytic motif. The amino acids essential for catalysis are known along with the phospho-transfer mechanism, mostly from the extensive characterization of PTP1B (PTP) (Barford et al., 1998). Using primary amino acid alignments of the catalytic domain of all Cdc14 orthologs and the comprehensively studied PTP1B we would begin by identifying residues that are not essential for catalysis but are largely conserved and may serve a minor catalytic role in orienting or stabilizing the substrate. These residues can be further analyzed using tertiary structure predictions to ensure that they are exposed and do not solely serve a structural purpose. These residues can be then used for individual and possibly combinatorial PCR based mutagenesis in budding yeast. The haploid progeny of mutants that confer a moderate growth defect will be then selected

for further characterization and ultimately for Cdc14 phospho-regulatory network analysis using SGA and 2D-DiGE.

In conclusion, we have shown that the use of a hypomorphic catalytic mutant, which is otherwise structurally intact thus conserving normal stochiometry and holoenzyme structure, is a novel tool for combinatory large scale genomic and proteomic screens. With our methodology regrouping genetic and protein data we identified a novel function for *ENO1* as a putative sensor linking energy requirements to the cell cycle, presumably perturbed in *glc7-E101Q* cells. Clearly, catalytically compromised PPase alleles can uncover novel interactions and further improve our understanding of the phospho-regulatory mechanism of the cell and its impact on vital cellular functions.

References

Anderson, C., and Tatchell, K. (2001). Hyperactive glycogen synthase mutants of Saccharomyces cerevisiae suppress the glc7-1 protein phosphatase mutant. J Bacteriol *183*, 821-829.

Andreassen, P. R., Lacroix, F. B., Villa-Moruzzi, E., and Margolis, R. L. (1998). Differential subcellular localization of protein phosphatase-1 alpha, gamma1, and delta isoforms during both interphase and mitosis in mammalian cells. J Cell Biol *141*, 1207-1215.

Andrews, P. D., and Stark, M. J. (2000). Type 1 protein phosphatase is required for maintenance of cell wall integrity, morphogenesis and cell cycle progression in Saccharomyces cerevisiae. J Cell Sci *113 (Pt 3)*, 507-520.

Baker, S. H., Frederick, D. L., Bloecher, A., and Tatchell, K. (1997). Alanine-scanning mutagenesis of protein phosphatase type 1 in the yeast Saccharomyces cerevisiae. Genetics *145*, 615-626.

Barford, D. (1995). Protein phosphatases. Curr Opin Struct Biol *5*, 728-734.

Barford, D., Das, A. K., and Egloff, M. P. (1998). The structure and mechanism of protein phosphatases: insights into catalysis and regulation. Annu Rev Biophys Biomol Struct *27*, 133-164.

Barton, G. J., Cohen, P. T., and Barford, D. (1994). Conservation analysis and structure prediction of the protein serine/threonine phosphatases. Sequence similarity with diadenosine tetraphosphatase from Escherichia coli suggests homology to the protein phosphatases. Eur J Biochem *220*, 225-237.

Bishop, A. C., Buzko, O., and Shokat, K. M. (2001). Magic bullets for protein kinases. Trends Cell Biol *11*, 167-172.

Bloecher, A., and Tatchell, K. (1999). Defects in Saccharomyces cerevisiae protein phosphatase type I activate the spindle/kinetochore checkpoint. Genes Dev *13*, 517-522.

Bloecher, A., and Tatchell, K. (2000). Dynamic localization of protein phosphatase type 1 in the mitotic cell cycle of Saccharomyces cerevisiae. J Cell Biol *149*, 125-140.

Blom, N., Sicheritz-Ponten, T., Gupta, R., Gammeltoft, S., and Brunak, S. (2004). Prediction of post-translational glycosylation and phosphorylation of proteins from the amino acid sequence. Proteomics *4*, 1633-1649.

Boeke, J. D., LaCroute, F., and Fink, G. R. (1984). A positive selection for mutants lacking orotidine-5'-phosphate decarboxylase activity in yeast: 5-fluoro-orotic acid resistance. Mol Gen Genet *197*, 345-346.

Bollen, M. (2001). Combinatorial control of protein phosphatase-1. Trends Biochem Sci *26*, 426-431.

Bollen, M., and Stalmans, W. (1992). The structure, role, and regulation of type 1 protein phosphatases. Crit Rev Biochem Mol Biol *27*, 227-281.

Brachmann, C. B., Davies, A., Cost, G. J., Caputo, E., Li, J., Hieter, P., and Boeke, J. D. (1998). Designer deletion strains derived from Saccharomyces cerevisiae S288C: a useful set of strains and plasmids for PCR-mediated gene disruption and other applications. Yeast *14*, 115-132.

Breitkreutz, B. J., Stark, C., and Tyers, M. (2002). The GRID: The General Repository for Interaction Datasets. Genome Biol *3*, PREPRINT0013.

Breitkreutz, B. J., Stark, C., and Tyers, M. (2003). Osprey: a network visualization system. Genome Biol *4*, R22.

Cannon, J. F., Pringle, J. R., Fiechter, A., and Khalil, M. (1994). Characterization of glycogen-deficient glc mutants of Saccharomyces cerevisiae. Genetics *136*, 485-503.

Carlson, M. (1999). Glucose repression in yeast. Curr Opin Microbiol *2*, 202-207.

Ceulemans, H., and Bollen, M. (2004). Functional diversity of protein phosphatase-1, a cellular economizer and reset button. Physiol Rev *84*, 1-39.

Ceulemans, H., Stalmans, W., and Bollen, M. (2002). Regulator-driven functional diversification of protein phosphatase-1 in eukaryotic evolution. Bioessays *24*, 371-381.

Cheeseman, I. M., Anderson, S., Jwa, M., Green, E. M., Kang, J., Yates, J. R., 3rd, Chan, C. S., Drubin, D. G., and Barnes, G. (2002). Phospho-regulation of kinetochore-microtubule attachments by the Aurora kinase Ipl1p. Cell *111*, 163-172.

Chen, K. C., Calzone, L., Csikasz-Nagy, A., Cross, F. R., Novak, B., and Tyson, J. J. (2004). Integrative analysis of cell cycle control in budding yeast. Mol Biol Cell *15*, 3841-3862.

Cho, H. P., Liu, Y., Gomez, M., Dunlap, J., Tyers, M., and Wang, Y. (2005). The dual-specificity phosphatase CDC14B bundles and stabilizes microtubules. Mol Cell Biol *25*, 4541-4551.

Christianson, T. W., Sikorski, R. S., Dante, M., Shero, J. H., and Hieter, P. (1992). Multifunctional yeast high-copy-number shuttle vectors. Gene *110*, 119-122.

Cullen, P. J., Sabbagh, W., Jr., Graham, E., Irick, M. M., van Olden, E. K., Neal, C., Delrow, J., Bardwell, L., and Sprague, G. F., Jr. (2004). A signaling mucin at the head of the Cdc42- and MAPK-dependent filamentous growth pathway in yeast. Genes Dev *18*, 1695-1708.

Cullen, P. J., and Sprague, G. F., Jr. (2002). The Glc7p-interacting protein Bud14p attenuates polarized growth, pheromone response, and filamentous growth in Saccharomyces cerevisiae. Eukaryot Cell *1*, 884-894.

Cuschieri, L., Miller, R., and Vogel, J. (2006). Gamma-tubulin is required for proper recruitment and assembly of Kar9-Bim1 complexes in budding yeast. Mol Biol Cell *17*, 4420-4434.

D'Amours, D., and Amon, A. (2004). At the interface between signaling and executing anaphase--Cdc14 and the FEAR network. Genes Dev *18*, 2581-2595.

Davierwala, A. P., Haynes, J., Li, Z., Brost, R. L., Robinson, M. D., Yu, L., Mnaimneh, S., Ding, H., Zhu, H., Chen, Y., *et al.* (2005). The synthetic genetic interaction spectrum of essential genes. Nat Genet *37*, 1147-1152.

Decker, B. L., and Wickner, W. T. (2006). Enolase activates homotypic vacuole fusion and protein transport to the vacuole in yeast. J Biol Chem *281*, 14523-14528.

Dien, B. S., Peterson, M. S., and Srienc, F. (1994). Cell-cycle analysis of Saccharomyces cerevisiae. Methods Cell Biol *42 Pt B*, 457-475.

Dobbelaere, J., Gentry, M. S., Hallberg, R. L., and Barral, Y. (2003). Phosphorylation-dependent regulation of septin dynamics during the cell cycle. Dev Cell *4*, 345-357.

Dombek, K. M., Voronkova, V., Raney, A., and Young, E. T. (1999). Functional analysis of the yeast Glc7-binding protein Reg1 identifies a protein phosphatase type 1-binding motif as essential for repression of ADH2 expression. Mol Cell Biol *19*, 6029-6040.

Drees, B. L., Thorsson, V., Carter, G. W., Rives, A. W., Raymond, M. Z., Avila-Campillo, I., Shannon, P., and Galitski, T. (2005). Derivation of genetic interaction networks from quantitative phenotype data. Genome Biol *6*, R38.

Ducruet, A. P., Vogt, A., Wipf, P., and Lazo, J. S. (2005). Dual specificity protein phosphatases: therapeutic targets for cancer and Alzheimer's disease. Annu Rev Pharmacol Toxicol *45*, 725-750.

Dynlacht, B. D. (1997). Regulation of transcription by proteins that control the cell cycle. Nature *389*, 149-152.

Egloff, M. P., Cohen, P. T., Reinemer, P., and Barford, D. (1995). Crystal structure of the catalytic subunit of human protein phosphatase 1 and its complex with tungstate. J Mol Biol *254*, 942-959.

Egloff, M. P., Johnson, D. F., Moorhead, G., Cohen, P. T., Cohen, P., and Barford, D. (1997). Structural basis for the recognition of regulatory subunits by the catalytic subunit of protein phosphatase 1. Embo J *16*, 1876-1887.

Enjalbert, B., Nantel, A., and Whiteway, M. (2003). Stress-induced gene expression in Candida albicans: absence of a general stress response. Mol Biol Cell *14*, 1460-1467.

Enjalbert, B., Parrou, J. L., Vincent, O., and Francois, J. (2000). Mitochondrial respiratory mutants of Saccharomyces cerevisiae accumulate glycogen and readily mobilize it in a glucose-depleted medium. Microbiology *146 (Pt 10)*, 2685-2694.

Entian, K. D., Meurer, B., Kohler, H., Mann, K. H., and Mecke, D. (1987). Studies on the regulation of enolases and compartmentation of cytosolic enzymes in Saccharomyces cerevisiae. Biochim Biophys Acta *923*, 214-221.

Fauman, E. B., and Saper, M. A. (1996). Structure and function of the protein tyrosine phosphatases. Trends Biochem Sci *21*, 413-417.

Feng, Z. H., Wilson, S. E., Peng, Z. Y., Schlender, K. K., Reimann, E. M., and Trumbly, R. J. (1991). The yeast GLC7 gene required for glycogen accumulation encodes a type 1 protein phosphatase. J Biol Chem *266*, 23796-23801.

Ferea, T. L., Botstein, D., Brown, P. O., and Rosenzweig, R. F. (1999). Systematic changes in gene expression patterns following adaptive evolution in yeast. Proc Natl Acad Sci U S A *96*, 9721-9726.

Ferrari, S. (2006). Protein kinases controlling the onset of mitosis. Cell Mol Life Sci *63*, 781-795.

Francisco, L., and Chan, C. S. (1994). Regulation of yeast chromosome segregation by Ipl1 protein kinase and type 1 protein phosphatase. Cell Mol Biol Res *40*, 207-213.

Francois, J., and Parrou, J. L. (2001). Reserve carbohydrates metabolism in the yeast Saccharomyces cerevisiae. FEMS Microbiol Rev *25*, 125-145.

Gavin, A. C., Bosche, M., Krause, R., Grandi, P., Marzioch, M., Bauer, A., Schultz, J., Rick, J. M., Michon, A. M., Cruciat, C. M., *et al.* (2002). Functional organization of the yeast proteome by systematic analysis of protein complexes. Nature *415*, 141-147.

Gilbert, W., and Guthrie, C. (2004). The Glc7p nuclear phosphatase promotes mRNA export by facilitating association of Mex67p with mRNA. Mol Cell *13*, 201-212.

Gladfelter, A. S., Pringle, J. R., and Lew, D. J. (2001). The septin cortex at the yeast mother-bud neck. Curr Opin Microbiol *4*, 681-689.

Goldberg, J., Huang, H. B., Kwon, Y. G., Greengard, P., Nairn, A. C., and Kuriyan, J. (1995). Three-dimensional structure of the catalytic subunit of protein serine/threonine phosphatase-1. Nature *376*, 745-753.

Graumann, J., Dunipace, L. A., Seol, J. H., McDonald, W. H., Yates, J. R., 3rd, Wold, B. J., and Deshaies, R. J. (2004). Applicability of tandem affinity purification MudPIT to pathway proteomics in yeast. Mol Cell Proteomics *3*, 226-237.

Guex, N., and Peitsch, M. C. (1997). SWISS-MODEL and the Swiss-PdbViewer: an environment for comparative protein modeling. Electrophoresis *18*, 2714-2723.

Guillou, V., Plourde-Owobi, L., Parrou, J. L., Goma, G., and Francois, J. (2004). Role of reserve carbohydrates in the growth dynamics of Saccharomyces cerevisiae. FEMS Yeast Res *4*, 773-787.

Guthrie, C. a. F., G. R. (1991). Guide to Yeast Genetics and Molecular Biology Part B: New York: Academic Press).

Hanks, S. K. (2003). Genomic analysis of the eukaryotic protein kinase superfamily: a perspective. Genome Biol *4*, 111.

Haystead, T. A., Sim, A. T., Carling, D., Honnor, R. C., Tsukitani, Y., Cohen, P., and Hardie, D. G. (1989). Effects of the tumour promoter okadaic acid on intracellular protein phosphorylation and metabolism. Nature *337*, 78-81.

Hinnebusch, A. G., and Natarajan, K. (2002). Gcn4p, a master regulator of gene expression, is controlled at multiple levels by diverse signals of starvation and stress. Eukaryot Cell *1*, 22-32.

Hisamoto, N., Sugimoto, K., and Matsumoto, K. (1994). The Glc7 type 1 protein phosphatase of Saccharomyces cerevisiae is required for cell cycle progression in G2/M. Mol Cell Biol *14*, 3158-3165.

Ho, Y., Gruhler, A., Heilbut, A., Bader, G. D., Moore, L., Adams, S. L., Millar, A., Taylor, P., Bennett, K., Boutilier, K., *et al.* (2002). Systematic identification of protein complexes in Saccharomyces cerevisiae by mass spectrometry. Nature *415*, 180-183.

Holtz, K. M., Stec, B., and Kantrowitz, E. R. (1999). A model of the transition state in the alkaline phosphatase reaction. J Biol Chem *274*, 8351-8354.

Hsu, J. Y., Sun, Z. W., Li, X., Reuben, M., Tatchell, K., Bishop, D. K., Grushcow, J. M., Brame, C. J., Caldwell, J. A., Hunt, D. F., *et al.* (2000). Mitotic phosphorylation of histone H3 is governed by Ipl1/aurora kinase and Glc7/PP1 phosphatase in budding yeast and nematodes. Cell *102*, 279-291.

Hu, X. D., Huang, Q., Roadcap, D. W., Shenolikar, S. S., and Xia, H. (2006). Actin-associated neurabin-protein phosphatase-1 complex regulates hippocampal plasticity. J Neurochem *98*, 1841-1851.

Janssens, V., and Goris, J. (2001). Protein phosphatase 2A: a highly regulated family of serine/threonine phosphatases implicated in cell growth and signalling. Biochem J *353*, 417-439.

Johnson, L. N., and Lewis, R. J. (2001). Structural basis for control by phosphorylation. Chem Rev *101*, 2209-2242.

Johnson, L. N., and O'Reilly, M. (1996). Control by phosphorylation. Curr Opin Struct Biol *6*, 762-769.

Kiemer, L., Bendtsen, J. D., and Blom, N. (2005). NetAcet: prediction of N-terminal acetylation sites. Bioinformatics *21*, 1269-1270.

Kim, G., Sikder, H., and Singh, K. K. (2002). A colony color method identifies the vulnerability of mitochondria to oxidative damage. Mutagenesis *17*, 375-381.

Knaus, M., Cameroni, E., Pedruzzi, I., Tatchell, K., De Virgilio, C., and Peter, M. (2005). The Bud14p-Glc7p complex functions as a cortical regulator of dynein in budding yeast. Embo J *24*, 3000-3011.

Knop, M., Siegers, K., Pereira, G., Zachariae, W., Winsor, B., Nasmyth, K., and Schiebel, E. (1999). Epitope tagging of yeast genes using a PCR-based strategy: more tags and improved practical routines. Yeast *15*, 963-972.

Kozubowski, L., Panek, H., Rosenthal, A., Bloecher, A., DeMarini, D. J., and Tatchell, K. (2003). A Bni4-Glc7 phosphatase complex that recruits chitin synthase to the site of bud emergence. Mol Biol Cell *14*, 26-39.

Kuruma, H., Egawa, S., Oh-Ishi, M., Kodera, Y., and Maeda, T. (2005). Proteome analysis of prostate cancer. Prostate Cancer Prostatic Dis *8*, 14-21.

Laemmli, U. K. (1970). Cleavage of structural proteins during the assembly of the head of bacteriophage T4. Nature *227*, 680-685.

Lavoie, L., Band, C. J., Kong, M., Bergeron, J. J., and Posner, B. I. (1999). Regulation of glycogen synthase in rat hepatocytes. Evidence for multiple signaling pathways. J Biol Chem *274*, 28279-28285.

Lindvall, M. K., Pihko, P. M., and Koskinen, A. M. (1997). The binding mode of calyculin A to protein phosphatase-1. A novel spiroketal vector model. J Biol Chem *272*, 23312-23316.

Longtine, M. S., DeMarini, D. J., Valencik, M. L., Al-Awar, O. S., Fares, H., De Virgilio, C., and Pringle, J. R. (1996). The septins: roles in cytokinesis and other processes. Curr Opin Cell Biol *8*, 106-119.

Longtine, M. S., McKenzie, A., 3rd, Demarini, D. J., Shah, N. G., Wach, A., Brachat, A., Philippsen, P., and Pringle, J. R. (1998). Additional modules for versatile and economical PCR-based gene deletion and modification in Saccharomyces cerevisiae. Yeast *14*, 953-961.

MacKelvie, S. H., Andrews, P. D., and Stark, M. J. (1995). The Saccharomyces cerevisiae gene SDS22 encodes a potential regulator of the mitotic function of yeast type 1 protein phosphatase. Mol Cell Biol *15*, 3777-3785.

Maeda, T., Tsai, A. Y., and Saito, H. (1993). Mutations in a protein tyrosine phosphatase gene (PTP2) and a protein serine/threonine phosphatase gene (PTC1) cause a synthetic growth defect in Saccharomyces cerevisiae. Mol Cell Biol *13*, 5408-5417.

Martin, H., Flandez, M., Nombela, C., and Molina, M. (2005). Protein phosphatases in MAPK signalling: we keep learning from yeast. Mol Microbiol *58*, 6-16.

McAlister, L., and Holland, M. J. (1982). Targeted deletion of a yeast enolase structural gene. Identification and isolation of yeast enolase isozymes. J Biol Chem *257*, 7181-7188.

McGuffin, L. J., Bryson, K., and Jones, D. T. (2000). The PSIPRED protein structure prediction server. Bioinformatics *16*, 404-405.

Mumby, M. C., and Walter, G. (1993). Protein serine/threonine phosphatases: structure, regulation, and functions in cell growth. Physiol Rev *73*, 673-699.

Myles, T., Schmidt, K., Evans, D. R., Cron, P., and Hemmings, B. A. (2001). Active-site mutations impairing the catalytic function of the catalytic subunit of human protein phosphatase 2A permit baculovirus-mediated overexpression in insect cells. Biochem J *357*, 225-232.

Nigavekar, S. S., Tan, Y. S., and Cannon, J. F. (2002). Glc8 is a glucose-repressible activator of Glc7 protein phosphatase-1. Arch Biochem Biophys *404*, 71-79.

Nolen, B., Taylor, S., and Ghosh, G. (2004). Regulation of protein kinases; controlling activity through activation segment conformation. Mol Cell *15*, 661-675.

Park, E. C., and Szostak, J. W. (1992). ARD1 and NAT1 proteins form a complex that has N-terminal acetyltransferase activity. Embo J *11*, 2087-2093.

Parrou, J. L., Teste, M. A., and Francois, J. (1997). Effects of various types of stress on the metabolism of reserve carbohydrates in Saccharomyces cerevisiae: genetic evidence for a stress-induced recycling of glycogen and trehalose. Microbiology *143 (Pt 6)*, 1891-1900.

Pawson, T. (1995). Protein modules and signalling networks. Nature *373*, 573-580.

Peggie, M. W., MacKelvie, S. H., Bloecher, A., Knatko, E. V., Tatchell, K., and Stark, M. J. (2002). Essential functions of Sds22p in chromosome stability and nuclear localization of PP1. J Cell Sci *115*, 195-206.

Pinsky, B. A., Kotwaliwale, C. V., Tatsutani, S. Y., Breed, C. A., and Biggins, S. (2006). Glc7/protein phosphatase 1 regulatory subunits can oppose the Ipl1/aurora protein kinase by redistributing Glc7. Mol Cell Biol *26*, 2648-2660.

Ptacek, J., Devgan, G., Michaud, G., Zhu, H., Zhu, X., Fasolo, J., Guo, H., Jona, G., Breitkreutz, A., Sopko, R., *et al.* (2005). Global analysis of protein phosphorylation in yeast. Nature *438*, 679-684.

Ramaswamy, N. T., Li, L., Khalil, M., and Cannon, J. F. (1998). Regulation of yeast glycogen metabolism and sporulation by Glc7p protein phosphatase. Genetics *149*, 57-72.

Roberts, G. G., and Hudson, A. P. (2006). Transcriptome profiling of Saccharomyces cerevisiae during a transition from fermentative to glycerol-based respiratory growth reveals extensive metabolic and structural remodeling. Mol Genet Genomics *276*, 170-186.

Robinson, M. D., Grigull, J., Mohammad, N., and Hughes, T. R. (2002). FunSpec: a web-based cluster interpreter for yeast. BMC Bioinformatics *3*, 35.

Romsicki, Y., Scapin, G., Beaulieu-Audy, V., Patel, S., Becker, J. W., Kennedy, B. P., and Asante-Appiah, E. (2003). Functional characterization and crystal structure of the C215D mutant of protein-tyrosine phosphatase-1B. J Biol Chem *278*, 29009-29015.

Saito, H., and Tatebayashi, K. (2004). Regulation of the osmoregulatory HOG MAPK cascade in yeast. J Biochem (Tokyo) *136*, 267-272.

Sakumoto, N., Matsuoka, I., Mukai, Y., Ogawa, N., Kaneko, Y., and Harashima, S. (2002). A series of double disruptants for protein phosphatase genes in Saccharomyces cerevisiae and their phenotypic analysis. Yeast *19*, 587-599.

Sakumoto, N., Mukai, Y., Uchida, K., Kouchi, T., Kuwajima, J., Nakagawa, Y., Sugioka, S., Yamamoto, E., Furuyama, T., Mizubuchi, H., *et al.* (1999). A series of protein phosphatase gene disruptants in Saccharomyces cerevisiae. Yeast *15*, 1669-1679.

Santangelo, G. M. (2006). Glucose signaling in Saccharomyces cerevisiae. Microbiol Mol Biol Rev *70*, 253-282.

Sanz, P., Alms, G. R., Haystead, T. A., and Carlson, M. (2000a). Regulatory interactions between the Reg1-Glc7 protein phosphatase and the Snf1 protein kinase. Mol Cell Biol *20*, 1321-1328.

Sanz, P., Ludin, K., and Carlson, M. (2000b). Sip5 interacts with both the Reg1/Glc7 protein phosphatase and the Snf1 protein kinase of Saccharomyces cerevisiae. Genetics *154*, 99-107.

Saunders, W. S. (2002). The FEAR factor. Mol Cell *9*, 207-209.

Sikorski, R. S., and Hieter, P. (1989). A system of shuttle vectors and yeast host strains designed for efficient manipulation of DNA in Saccharomyces cerevisiae. Genetics *122*, 19-27.

Stark, M. J. (1996). Yeast protein serine/threonine phosphatases: multiple roles and diverse regulation. Yeast *12*, 1647-1675.

Stasyk, T., Morandell, S., Bakry, R., Feuerstein, I., Huck, C. W., Stecher, G., Bonn, G. K., and Huber, L. A. (2005). Quantitative detection of phosphoproteins by combination of two-dimensional difference gel electrophoresis and phosphospecific fluorescent staining. Electrophoresis *26*, 2850-2854.

Stegmeier, F., and Amon, A. (2004). Closing mitosis: the functions of the Cdc14 phosphatase and its regulation. Annu Rev Genet *38*, 203-232.

Stuart, J. S., Frederick, D. L., Varner, C. M., and Tatchell, K. (1994). The mutant type 1 protein phosphatase encoded by glc7-1 from Saccharomyces cerevisiae fails to interact productively with the GAC1-encoded regulatory subunit. Mol Cell Biol *14*, 896-905.

Terrak, M., Kerff, F., Langsetmo, K., Tao, T., and Dominguez, R. (2004). Structural basis of protein phosphatase 1 regulation. Nature *429*, 780-784.

Thornton, B. R., and Toczyski, D. P. (2006). Precise destruction: an emerging picture of the APC. Genes Dev *20*, 3069-3078.

Tong, A. H., Evangelista, M., Parsons, A. B., Xu, H., Bader, G. D., Page, N., Robinson, M., Raghibizadeh, S., Hogue, C. W., Bussey, H., *et al.* (2001). Systematic genetic analysis with ordered arrays of yeast deletion mutants. Science *294*, 2364-2368.

Tong, A. H., Lesage, G., Bader, G. D., Ding, H., Xu, H., Xin, X., Young, J., Berriz, G. F., Brost, R. L., Chang, M., *et al.* (2004). Global mapping of the yeast genetic interaction network. Science *303*, 808-813.

Tu, J., and Carlson, M. (1995). REG1 binds to protein phosphatase type 1 and regulates glucose repression in Saccharomyces cerevisiae. Embo J *14*, 5939-5946.

Unlu, M., Morgan, M. E., and Minden, J. S. (1997). Difference gel electrophoresis: a single gel method for detecting changes in protein extracts. Electrophoresis *18*, 2071-2077.

Van Hoof, C., and Goris, J. (2003). Phosphatases in apoptosis: to be or not to be, PP2A is in the heart of the question. Biochim Biophys Acta *1640*, 97-104.

Ventura, J. J., and Nebreda, A. R. (2006). Protein kinases and phosphatases as therapeutic targets in cancer. Clin Transl Oncol *8*, 153-160.

Versele, M., and Thorner, J. (2004). Septin collar formation in budding yeast requires GTP binding and direct phosphorylation by the PAK, Cla4. J Cell Biol *164*, 701-715.

Vogel, J., Drapkin, B., Oomen, J., Beach, D., Bloom, K., and Snyder, M. (2001). Phosphorylation of gamma-tubulin regulates microtubule organization in budding yeast. Dev Cell *1*, 621-631.

Wan, J., Xu, H., and Grunstein, M. (1992). CDC14 of Saccharomyces cerevisiae. Cloning, sequence analysis, and transcription during the cell cycle. J Biol Chem *267*, 11274-11280.

Wek, R. C., Cannon, J. F., Dever, T. E., and Hinnebusch, A. G. (1992). Truncated protein phosphatase GLC7 restores translational activation of GCN4 expression in yeast mutants defective for the eIF-2 alpha kinase GCN2. Mol Cell Biol *12*, 5700-5710.

Williams-Hart, T., Wu, X., and Tatchell, K. (2002). Protein phosphatase type 1 regulates ion homeostasis in Saccharomyces cerevisiae. Genetics *160*, 1423-1437.

Winzeler, E. A., Shoemaker, D. D., Astromoff, A., Liang, H., Anderson, K., Andre, B., Bangham, R., Benito, R., Boeke, J. D., Bussey, H., *et al.* (1999). Functional characterization of the S. cerevisiae genome by gene deletion and parallel analysis. Science *285*, 901-906.

Wu, X., Hart, H., Cheng, C., Roach, P. J., and Tatchell, K. (2001). Characterization of Gac1p, a regulatory subunit of protein phosphatase type I involved in glycogen accumulation in Saccharomyces cerevisiae. Mol Genet Genomics *265*, 622-635.

Wu, X., and Tatchell, K. (2001). Mutations in yeast protein phosphatase type 1 that affect targeting subunit binding. Biochemistry *40*, 7410-7420.

Wurgler-Murphy, S. M., Maeda, T., Witten, E. A., and Saito, H. (1997). Regulation of the Saccharomyces cerevisiae HOG1 mitogen-activated protein kinase by the PTP2 and PTP3 protein tyrosine phosphatases. Mol Cell Biol *17*, 1289-1297.

Xue, Y., Zhou, F., Fu, C., Xu, Y., and Yao, X. (2006). SUMOsp: a web server for sumoylation site prediction. Nucleic Acids Res *34*, W254-257.

Yokota, T., Nara, Y., Kashima, A., Matsubara, K., Misawa, S., Kato, R., and Sugio, S. (2006). Crystal structure of human dual specificity phosphatase, JNK stimulatory phosphatase-1, at 1.5 A resolution. Proteins.

Zhan, X. L., and Guan, K. L. (1999). A specific protein-protein interaction accounts for the in vivo substrate selectivity of Ptp3 towards the Fus3 MAP kinase. Genes Dev *13*, 2811-2827.

Zhao, Y., Boguslawski, G., Zitomer, R. S., and DePaoli-Roach, A. A. (1997). Saccharomyces cerevisiae homologs of mammalian B and B' subunits of protein phosphatase 2A direct the enzyme to distinct cellular functions. J Biol Chem *272*, 8256-8262.

Zhu, H., Bilgin, M., Bangham, R., Hall, D., Casamayor, A., Bertone, P., Lan, N., Jansen, R., Bidlingmaier, S., Houfek, T., *et al.* (2001). Global analysis of protein activities using proteome chips. Science *293*, 2101-2105.

Zhuo, S., Clemens, J. C., Stone, R. L., and Dixon, J. E. (1994). Mutational analysis of a Ser/Thr phosphatase. Identification of residues important in phosphoesterase substrate binding and catalysis. J Biol Chem *269*, 26234-26238.

Appendix

Figure S1: PSIPRED: the C-terminus of Glc7 is disordered

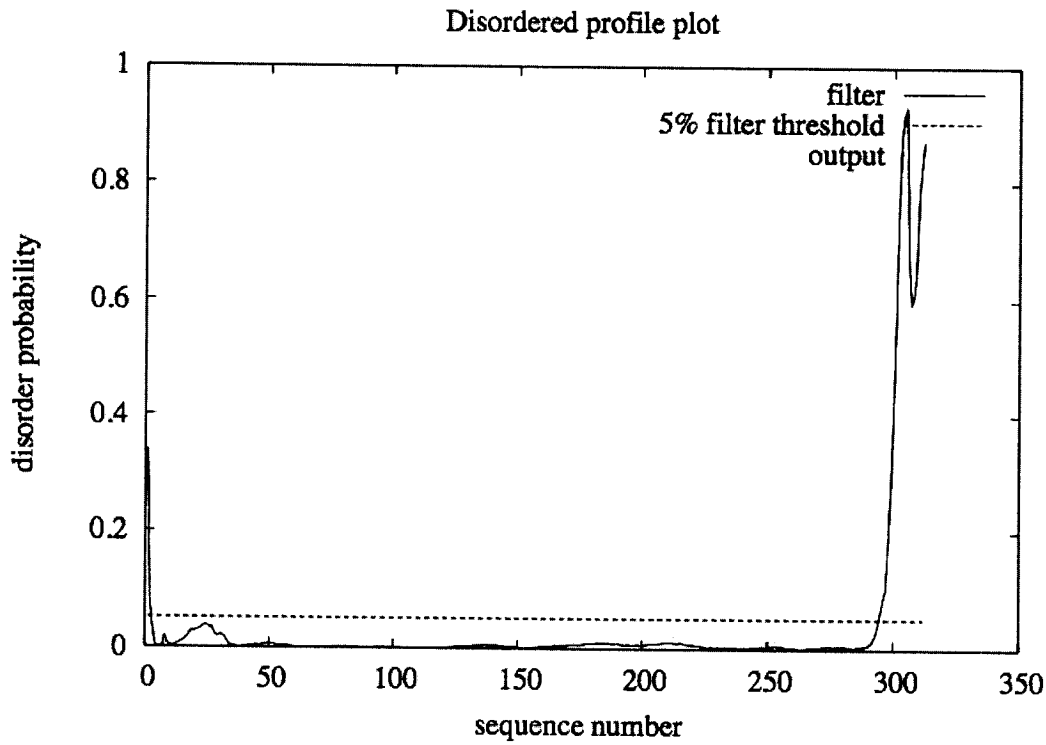

Table S1: List of forward *GLC7* mutagenic primers

Primer	Sequence 5'-3'	Predicted activity	References
Glc7 D91N_AvrII F	GATTCCCGCCAGAATCTAAT TATCTATT*ccTaGGT*aATTATG TCGACCGTGGTAAACAATCC TTAGAGAC	Very low to none	(Egloff et al., 1995; Egloff et al., 1997; Goldberg et al., 1995)
Glc7 D94N_AvrII F	GATTCCCGCCAGAATCTAAT TATCTATT*ccTaGG*TGATTATG TCaACCGTGGTAAACAATCC TTAGAGAC	Very low to none	(Egloff et al., 1997; Goldberg et al., 1995; Myles et al., 2001)
Glc7 R95A_AvrII F	GATTCCCGCCAGAATCTAAT TATCTATT*ccTaGG*TGATTATG TCGACgcTGGTAAACAATCCT TAGAGAC	Low	(Egloff et al., 1995; Egloff et al., 1997; Lindvall et al., 1997; Myles et al., 2001)
Glc7 E101Q_HindIII F	TGGGTGATTATGTCGACCGT GGTAAACA*AagCTT*AcAGACT ATTTGTCTATTACTGGCTT	Low	(Zhuo et al., 1994)
Glc7 R121A_Nhe I F	GAGACTATTTGTCTATT*gCTa GC*TTACAAAATTAAGTATCCA GAAAACTTTTTCATTTTAgcA GGGAACCATGAA	Low	(Myles et al., 2001; Zhuo et al., 1994)
Glc7 E125Q_AflII F	GTATCCAGAAAACTTTTTCAT *cTTAAG*AGGGAACCATcAATG TGCTTCCATTAATAGAAT	Very low to none	(Zhuo et al., 1994)

List of forward *GLC7* mutagenic primers with predicted reduction in catalytic activity. The altered codon for the amino acid switch is underlined, capitalized sequence indicates homology to *GLC7* genomic DNA and italics indicate a restriction site.

Table S2. Additional primers for mutagenesis and cloning of *GLC7*

Primer	Sequence 5'-3'	Template	Comment
Glc7_PL_ProA_R	TGTTAATAAGTATTTT CCTTTTTAAACTTTGA TTTAGGACGTGAATCT ATttaaactggatggcggcgtt ag	pGLC7-2	Used with primers from table S1 to create C-terminal epitope tagged alleles of Glc7
Glc7_PL_KanMX_ R	CACATCTTATTATTAT CTCCTTTTTTTTATATT TTTTTTATGTTTCTTATt taaactggatggcggcgttag	pGLC7-1	Used with primers from table S1 to create untagged alleles of Glc7
Glc7_NAT_R	CACATCTTATTATTAT CTCCTTTTTTTTATATT TTTTTTATGTTTCTTAT cagtatagcgaccagcattcac	Genomic	Used with primers from table S1 to create the SGA strain
Glc7 Test F	GAAATGTGGATTTGCA GAAG	Genomic	Test Primer
Glc7 Test R	TCACCCTTCTGATCTG TTCC	Genomic	Test Primer
GLC7 F	ctaagctatt*ggtacc*TTATG TTTTGTATCATCATCC	Genomic	Forward cloning primer used for constructing pGLC7-1 and -2
GLC7-1.0 R	gtatcgtcaa*gcggccgc*TTT TTTCTTTCTACCCCCA GCTTG	Genomic	Reverse cloning primer used for constructing pGLC7-2
GLC7-1.2 R	gtatcgtcaa*gcggccgc*TTC GCGGTTTGTTGCACTA AAGGG	Genomic	Reverse cloning primer used for constructing pGLC7-1
GLC7-full F	ctaagctatt*ggtacc*GTTAT TCAATTGAGGTAGATA CC	Genomic	Forward cloning primer used for constructing pGLC7-3
GLC7-full R	atgatcgatg*gagctc*CTTAT CATTTTTCCACTAATT CAAATCC	Genomic	Reverse cloning primer used for constructing pGLC7-3

Reverse primers for mutagenesis of *GLC7* and universal test primers along with the forward primer use to create the SGA query strain YNS98. *GLC7* cloning primers used to construct pGLC7-x are also included. Capitalized sequence indicates homology to *GLC7* genomic DNA and italics indicate a restriction site.

Table S3: List of synthetic sick/lethal (SSL) and synthetic rescue (SR) interactions with *glc7-E101Q*

GO term	Interaction	Gene/ORF
amino acid and derivative metabolism	SSL	ASN1, GDH1
	SR	AAT2, ARG2, ARG4, ARO7, CPA1, CYS3, CYS4, GCN4, HIS1, HIS2, HIS7, HOM3, HOM6, ILV1, LYS1, LYS12, LYS2, LYS4, LYS9, PHA2, SER1, SER2, TRP1, TRP2, TRP5
biological process unknown	SSL	EAF6, FMP35, RMD11, SPG5, TMA108, UTR4, YEL048C, YGL059W, YHR035W, YJR088C, YML053C, YMR144W, YMR253C, YNL191W, YNL300W, YNL320W, YOR289W, YPR147C
	SR	AMD2, FMP42, MRN1, OYE3, PCS60, RMD9, UBP13, YBL095W, YBR225W, YDL057W, YDL206W, YDR114C, YGR150C, YLR356W, YOR097C, YPR116W
carbohydrate metabolism	SSL	GLO2, RPE1
	SR	ENO1
cell budding	SSL	URM1
	SR	AXL2, BUD4, GIN4
cell cycle	SSL	BIR1, CTF18, NIP100, JNM1, SAP155, SWI5
	SR	PHO85
cell homeostasis	SSL	CKB2, PPZ1
	SR	TRK1
cell wall organization and biogenesis	SSL	ECM5, ECM8, KRE1, KTR3
	SR	GET2, SIT4
cellular respiration	SR	COX20, KGD2, YDR115W
conjugation	SSL	FAR7
	SR	MOT2, SCW10
cytokinesis	SSL	CLA4
	SR	BUD25, END3
cytoskeleton organization and biogenesis	SSL	ACF4, KAR9
	SR	BIM1, NAT3
DNA metabolism	SSL	DST1, EXO1, MUM2, NUP133, RAD14, RRD1, THP1, UNG1, YAF9
	SR	MIP1, RPH1, RSC2, SNF2, SNF5, SOH1
generation of precursor	SSL	RPE1

metabolites and energy	SR	ATP4, GPH1, VMA22
lipid metabolism	SSL	HFA1, OPI3, PSD1, YBR042C
	SR	CEM1, ERG28, ERG5, INO2, INO4
meiosis	SSL	CIK1, DST1, KAR3, REC8, TOR1
	SR	ALK2, DOT1, SPO13, SWI6
membrane organization and biogenesis	SSL	CYC2
	SR	PEP5, VAC8, VTC1
morphogenesis	SSL	KAP122
nuclear organization and biogenesis	SSL	NUP188
	SR	NUP53
organelle organization and biogenesis	SSL	ABF2, ANT1, INP2, MRC1, SWA2, YOL138C
	SR	ARG2, CUP5, LDB19, MST27, PEP5, PEX3, PEX6, RIM1, TRK1, VAC8, VPS3, VTC1, YGR042W
protein biosynthesis	SSL	CBP6, HCR1, IMG1, MET13, PAT1, RPL20A, RPL37A, RPL6B, RPL9B, RPP1A, RPS16A, RPS17A, RPS19A, RPS1A, RPS25A, RTS1
	SR	CAF20, IFM1, MRPL6, MSE1, MSK1, MSM1, RML2, RPL12A, RPL24A, RSM18, RSM27, YOR302W
protein catabolism	SSL	DER1, SEL1
	SR	CUL3
protein modification	SSL	CKB2, SIN3, URM1
	SR	ADA2, ANP1, ARD1, CDC26, COX20, GIN4, IMP1, LYS5, MAK10, MAK3, NGG1, OTU1, PFA5, PPM1, SAK1, SPF1, UBP3
pseudohyphal growth	SSL	GPA2, MSS11
	SR	NPL3
response to stress	SSL	CKB2, CTF8, DCC1, GET3, RRD1, SCO1, SIP5, WHI2, YIM1, ZWF1
	SR	GLR1, KCS1, POS5, RFX1, RPB9, UMP1
ribosome biogenesis and assembly	SSL	MRT4, YBL054W
	SR	PRS3
RNA metabolism	SSL	CBC2, ELP2, ELP3, KTI12, LSM1, LSM12, LSM6, MRS4, REX2, TRF5
	SR	CDC40, UPF3
signal transduction	SSL	BAG7, GPA2, TOR1
	SR	STD1
sporulation	SSL	SMA2
	SR	SPS18
Transcription	SSL	CTH1, HAP2, LEU3, SUM1, SWI5,

Transcription		TYE7, UGA3
	SR	ARG5,6, CHD1, DAL81, GAL11, GLN3, INO2, INO4, MTF1, OTU1, SWI6
transport	SSL	ARL3, ATG5, AVT5, BAP2, FPS1, MCH4, MID1, MIR1, MRS4, VPS73, VPS9, YNR070W
	SR	ADP1, AGP3, CAN1, CCS1, COX19, ENB1, SEC28, SMF1, SNF8, SXM1, VMA22, VMA7, VMA8, VPH2, VPS25, YKR078W
vesicle-mediated transport	SSL	SEM1
	SR	CUP5, DID4, ENT5, FTH1, PEP5, SEC28

Table S4: Mass spectrometry and database search results (Mascot)

Spot	(Accession) Protein	Observed Mass	Mr (expt)	Mr (calc)	Score Coverage	Rank	Peptide Sequence
Eno1 A	(119336) Enolase 1	407.93	813.85	813.5	51	1	AADALLLK
Eno1 A	(119336) Enolase 1	550.75	1099.48	1099.52	47	1	DGKYDLDFK
Eno1 A	(119336) Enolase 1	580.28	1158.55	1158.6	47	1	IGSEVYHNLK
Eno1 A	(119336) Enolase 1	387.43	1159.26	1158.6	34	1	IGSEVYHNLK
Eno1 A	(119336) Enolase 1	643.87	1285.73	1285.7	37	1	**NVNDVIAPA FVK**
Eno1 A	(119336) Enolase 1	645.06	1288.1	1287.7	29	1	VNQIGTLSESI K
Eno1 A	(119336) Enolase 1	687.93	1373.85	1372.63	8	3	IGLDCASSEF FK
Eno1 A	(119336) Enolase 1	708.76	1415.5	1415.71	61	1	GNPTVEVELT TEK
Eno1 A	(119336) Enolase 1	708.94	1415.86	1415.71	45	1	GNPTVEVELT TEK
Eno1 A	(119336) Enolase 1	749.41	1496.8	1496.84	42	1	NVPLYKHLA DLSK
Eno1 A	(119336) Enolase 1	500.19	1497.54	1496.84	11	1	NVPLYKHLA DLSK
Eno1 A	(119336) Enolase 1	790.39	1578.77	1577.79	54	1	AVDDFLISLD GTANK
Eno1 A	(119336) Enolase 1	619.99	1856.94	1855.91	42	1	SIVPSGASTG VHEALEMR + Oxidation (M)
Eno1 B	(119336) Enolase 1	404.27	806.52	806.43	44	1	**TFAEALR**
Eno1 B	(119336) Enolase 1	407.79	813.57	813.5	43	1	AADALLLK
Eno1 B	(119336) Enolase 1	471.77	941.52	941.59	50	1	KAADALLLK
Eno1 B	(119336) Enolase 1	550.72	1099.42	1099.52	52	1	DGKYDLDFK
Eno1 B	(119336) Enolase 1	367.54	1099.6	1099.52	34	1	DGKYDLDFK
Eno1 B	(119336) Enolase 1	580.25	1158.49	1158.6	46	1	IGSEVYHNLK
Eno1 B	(119336) Enolase 1	387.18	1158.53	1158.6	36	1	IGSEVYHNLK
Eno1 B	(119336) Enolase 1	643.83	1285.65	1285.7	54	1	**NVNDVIAPA FVK**
Eno1 B	(119336) Enolase 1	644.8	1287.59	1287.7	55	1	VNQIGTLSESI K
Eno1 B	(119336) Enolase 1	687.63	1373.25	1372.63	73	1	IGLDCASSEF FK

Eno1 B	(119336) Enolase 1	708.78	1415.54	1415.71	66	1	GNPTVEVELT TEK
Eno1 B	(119336) Enolase 1	708.89	1415.76	1415.71	61	1	GNPTVEVELT TEK
Eno1 B	(119336) Enolase 1	485.91	1454.72	1454.67	44	1	**YDLDFKNPN SDK**
Eno1 B	(119336) Enolase 1	789.78	1577.54	1577.79	67	1	AVDDFLISLD GTANK
Eno1 B	(119336) Enolase 1	526.93	1577.76	1577.79	90	1	AVDDFLISLD GTANK
Eno1 B	(119336) Enolase 1	878.53	1755.05	1754.94	94	1	**TAGIQIVAD DLTVTNPK**
Eno1 B	(119336) Enolase 1	920.84	1839.66	1839.91	124	1	SIVPSGASTG VHEALEMR
Eno1 B	(119336) Enolase 1	619.56	1855.67	1855.91	41	1	SIVPSGASTG VHEALEMR + Oxidation (M)
Eno1 B	(119336) Enolase 1	708.78	2123.31	2123.04	59	1	SVYDSRGNPT VEVELTTEK
Eno1 B	(119336) Enolase 1	814.31	2439.92	2440.13	77	1	**IEEELGDNA VFAGENFHH GDKL**
Eno1 C	(119336) Enolase 1	407.73	813.44	813.50	44	1	AADALLLK
Eno1 C	(119336) Enolase 1	387.13	1158.38	1158.60	10	1	IGSEVYHNLK
Eno1 C	(119336) Enolase 1	580.24	1158.46	1158.60	43	1	IGSEVYHNLK
Eno1 C	(119336) Enolase 1	387.19	1158.54	1158.60	26	1	IGSEVYHNLK
Eno1 C	(119336) Enolase 1	643.89	1285.76	1285.70	41	1	**NVNDVIAPA FVK**
Eno1 C	(119336) Enolase 1	644.88	1287.75	1287.70	70	1	VNQIGTLSESI K
Eno1 C	(119336) Enolase 1	687.48	1372.95	1372.63	87	1	IGLDCASSEF FK
Eno1 C	(119336) Enolase 1	708.80	1415.59	1415.71	59	1	GNPTVEVELT TEK
Eno1 C	(119336) Enolase 1	789.81	1577.61	1577.79	110	1	AVDDFLISLD GTANK
Eno1 C	(119336) Enolase 1	878.46	1754.91	1754.94	118	1	**TAGIQIVAD DLTVTNPK**
Eno1 C	(119336) Enolase 1	614.39	1840.16	1839.91	69	1	SIVPSGASTG VHEALEMR
Eno1 C	(119336) Enolase 1	619.68	1856.02	1855.91	39	1	SIVPSGASTG VHEALEMR + Oxidation (M)

Mascot output of peptides identified by LC-MS/MS (QTRAP) from excised spots Eno1_A, Eno1_B and Eno1_C respectively, matched to Enolase 1. Scores above 30 ($p<0.05$) are statistically significant. Eno1 unique peptides are in bold.